NASA TECHNICAL NOTE

NASA TN D-5663

c. 1

NASA TN D-5663

ANALYTICAL VIBRATION STUDY OF A RING-STIFFENED CONICAL SHELL AND COMPARISON WITH EXPERIMENT

by John L. Sewall and Donnell S. Catherines

Langley Research Center
Langley Station, Hampton, Va.

NATIONAL AERONAUTICS AND SPACE ADMINISTRATION • WASHINGTON, D. C. • FEBRUARY 1970

Completed
20 Oct 70 SW

ERRATA

NASA Technical Note D-5663

ANALYTICAL VIBRATION STUDY OF A RING-STIFFENED CONICAL SHELL AND COMPARISON WITH EXPERIMENT

By John L. Sewall and Donnell S. Catherines

February 1970

Page 15, line 9 of first paragraph: Change the word "spot-welds" to the word "bonding."

Page 16, line 9 of second paragraph: Change $n = 4$ and 5 to $n = 3$ and 4.

Page 43, figure 1(b): In the upper portion of the figure, change the word "spot-welds" to the word "bonding."

Page 49, figure 5(a): In left column of plots, change the integers 6, 5, and 4 to 5, 4, and 3, respectively.

NASA-Langley, 1970

Issued 10-13-70

1. Report No. NASA TN D-5663	2. Government Accession No.	3. Recipient's Catalog No.
4. Title and Subtitle ANALYTICAL VIBRATION STUDY OF A RING-STIFFENED CONICAL SHELL AND COMPARISON WITH EXPERIMENT		5. Report Date February 1970 6. Performing Organization Code
7. Author(s) John L. Sewall and Donnell S. Catherines		8. Performing Organization Report No. L-6747 10. Work Unit No. 124-08-13-04-23
9. Performing Organization Name and Address NASA Langley Research Center Hampton, Va. 23365		11. Contract or Grant No. 13. Type of Report and Period Covered Technical Note
12. Sponsoring Agency Name and Address National Aeronautics and Space Administration Washington, D.C. 20546		14. Sponsoring Agency Code

15. Supplementary Notes

16. Abstract

A Rayleigh-Ritz vibration analysis employing the concept of chosen modes is described and applied to a ring-stiffened, truncated, clamped-free, conical shell for which experimental vibration data are available for comparison. Power-series functions are employed to approximate meridional components of the in-plane and normal displacements, and the rings are treated as discrete elements of arbitrary cross section. In addition to the primary extensional and bending stiffnesses of the ring, together with its mass and centroid location inside or outside the shell wall, other so-called secondary stiffnesses and inertias are included to account for out-of-plane bending, cross-sectional asymmetry, warping, rotatory inertia, and the meridional centroid position relative to the ring attachment point. Good agreement between experimental and analytical frequencies and mode shapes was obtained for the shell with a ring of rectangular cross section attached near the clamped end and with rings of Z-shaped cross section attached at different stations along the shell meridian.

17. Key Words Suggested by Author(s) Vibration Ring-stiffened conical shell Reentry structures	18. Distribution Statement Unclassified – Unlimited

19. Security Classif. (of this report) Unclassified	20. Security Classif. (of this page) Unclassified	21. No. of Pages 57	22. Price* $3.00

*For sale by the Clearinghouse for Federal Scientific and Technical Information Springfield, Virginia 22151

ANALYTICAL VIBRATION STUDY OF A RING-STIFFENED CONICAL SHELL AND COMPARISON WITH EXPERIMENT

By John L. Sewall and Donnell S. Catherines
Langley Research Center

SUMMARY

A Rayleigh-Ritz vibration analysis employing the concept of chosen modes is described and applied to a ring-stiffened, truncated conical shell for which experimental vibration data are available for comparison. Simple power-series functions are employed to approximate meridional components of the in-plane and normal displacements for free-free and clamped-free end conditions. For the clamped-free shell, the series functions satisfy displacement boundary conditions for a conical-shell frustum clamped at the small end and free at the large end. Rings are treated as discrete elements of arbitrary cross section. In addition to the primary extensional and bending stiffnesses of the ring, together with its mass and centroid location inside or outside the shell wall, other so-called secondary stiffnesses and inertias are included to account for out-of-plane bending, cross-sectional asymmetry (product of inertia), warping, rotatory inertia, and the meridional centroid position relative to the ring attachment point.

Good agreement between analytical and experimental frequencies and mode shapes was obtained for the shell with a ring of rectangular cross section attached near the clamped end and with rings of Z-shaped cross section attached at different stations along the shell meridian. Analytical results were converged with 12 power-series modal functions approximating the meridional component of the normal displacement (or w) for the shell without Z-rings, 16 w-terms for the shell with a Z-ring attached to the free end, and 17 w-terms for the shell with an additional Z-ring midway along the meridian. Agreement was best for the shell without Z-rings and was better for the model with the Z-ring at the free end than for the model with two Z-rings. Agreement was also better for circumferential modes where shell effects predominated.

For circumferential modes where ring effects predominated, in some instances secondary stiffnesses and inertias caused changes in frequency of over 40 percent and correspondingly large changes in mode shape. The modes where shell effects predominated were negligibly affected by these added terms for the single-ring shell, and only a small increase in frequencies was noted for the two-ring shell.

INTRODUCTION

Various structural dynamics problems have been encountered in rocket nozzles and interstage launch-vehicle structures during the past several years and are anticipated in planetary entry vehicles. These problems have stimulated considerable interest in dynamic studies of conical-shell configurations which are among the basic components of these aerospace structures. Numerous vibration studies have been made for conical shells, and some of these are reported in references 1 to 6 for thin reinforced shells having semivertex angles of 20° or less. Motivation for investigating the vibrations of shells of wider cone angles has come largely from the requirements of large, blunt-body, lightweight structures for entry into sparse planetary atmospheres. Reference 7 and the present paper report vibration studies of thin-shell conical frustums with semivertex angles of as much as 60°.

The main purpose of the present paper is to demonstrate the use of a linear Rayleigh-Ritz analysis in calculating the vibration modes of a 60° ring-stiffened, conical-shell frustum. Experimental vibration modes obtained in an unpublished study by Eugene C. Naumann, John S. Mixson, and Earl C. Steeves of the Langley Research Center are compared with analytical vibration modes of the present analysis for the shell structure without payload mass. Another purpose of the paper is an evaluation of the effects of out-of-plane bending, cross-sectional asymmetry, warping, and rotatory inertia of the stiffener. The ring stiffeners are treated as discrete elements with their stiffness and mass properties lumped at the meridional ring locations. Circumferential components of in-plane and normal displacements are each expressed by single-term trigonometric functions, and meridional components are each expressed by a selected number of power-series functions. The analysis is essentially the same as that of reference 7 except for the choice of different power-series expansion functions.

Comparisons between results of the present analysis and the previously noted unpublished study include not only the shell stiffened by Z-shaped rings but also the shell stiffened by a "base" ring of rectangular cross section (close to the small end of the shell) and the free Z-rings. Following the general development of the frequency equations for the shell-ring combination and the free ring, the application of the analysis is demonstrated first for the base-ring configuration and next for the shell with Z-rings. Pertinent details of the analytical development in the main text are given in three appendixes which include a derivation of the ring strain-displacement relations and listings of the matrix elements.

SYMBOLS

A, B, E, F, G, H	primary stiffness submatrices
$\Delta A_{jm,R}, \Delta B_{jm,R}, \Delta E_{jm,R}, \Delta G_{jm,R}, \Delta H_{jm,R}$	secondary stiffness and eccentricity contributions to ring stiffness matrix elements (see appendix B)
A_R	ring cross-sectional area
$a_m(t), a_j(t)$	meridional in-plane generalized coordinates of shell
$b_m(t), b_j(t)$	circumferential in-plane generalized coordinates of shell
$c_m(t), c_j(t)$	radial (or normal) generalized coordinates of shell
E_c, E_R	Young's modulus of shell and ring, respectively
f	circular frequency, $\omega/2\pi$, Hz
G_R	shear modulus of ring
h	shell thickness
$I_{os,R}$	moment of inertia of ring about its centroidal axis parallel to s-axis
$I_{oz,R}$	moment of inertia of ring about its centroidal axis parallel to z-axis
$I_{s,R}$	moment of inertia of ring about $\hat{s}$-axis (eq. (9a))
$I_{z,R}$	moment of inertia of ring about $\hat{z}$-axis (eq. (9b))
$I_{sz,R}$	product of inertia of ring with respect to $\hat{s}$- and $\hat{z}$-axes (eqs. (8))
$I_{1,R}, I_{2,R}$	other moments of inertia defined in equations (8)
$I_1, I_2, \ldots, I_{14}$	integrals based on power series (appendix B)
$i = \sqrt{-1}$	

$J_{e,R}$ polar moment of inertia of ring cross section (defined by equation following equation (15))

J_R torsional constant of ring

j, m integers associated with meridional modes

$K_{11} \ldots K_{44}$, $M_{11} \ldots M_{44}$ elements of stiffness and mass matrices of free-ring frequency equation (eq. (20) and appendix C)

k, M integers identifying number of rings

L meridional length of shell between ends, $s_2 - s_1$

n number of circumferential waves

P, Q integers identifying bounds of truncated series (eqs. (16))

r shell radius (fig. 1(a))

r_0 average radius of truncated conical shell, $(r_1 + r_2)/2$

r_1 radius of small end of shell

r_2 radius of large end of shell

s meridional coordinate (fig. 1(a))

s_1 meridional distance from apex of cone to small end of cone (fig. 1(a))

s_2 meridional distance from apex of cone to large end of cone (fig. 1(a))

$\hat{s}_R$ meridional distance from $\hat{z}$-axis to ring centroid, positive toward large end of shell (fig. 1(a))

T kinetic energy

ΔT_R kinetic energy based on rotatory inertia terms in rings (eq. (15))

t	time
U	strain energy
ΔU_R	strain energy based on secondary stiffness terms in rings (eq. (7))
u, v, w	in-plane and normal displacements (fig. 1(a))
$\bar{u}, \bar{v}, \bar{w}$	in-plane and normal displacements of ring in $\hat{\phi}$-$\hat{z}$ plane (see appendix A)
$X(s)$	meridional mode shape (eqs. (16))
z	normal coordinate (fig. 1(a))
z_R	distance from shell middle surface to ring centroid, positive outward
α, β, γ	dominant mass submatrices
$\alpha\beta, \alpha\gamma, \beta\gamma$	rotatory inertia contributions to ring mass submatrices
β_R	free-ring twist about elastic axis
Γ_R	ring warping constant (see eqs. (8))
δ	semivertex angle of shell
$\epsilon_{11}, \epsilon_{22}, \epsilon_{12}$	membrane strain-displacement relations (see eqs. (1a), (1b), and (1c))
$\kappa_{11}, \kappa_{22}, \bar{\kappa}_{12}$	bending and torsion strain-displacement relations (see eqs. (1d), (1e), and (1f))
μ	Poisson's ratio for shell
ρ	mass density
ϕ	circumferential coordinate (see fig. 1(a))
$\phi_{1,R}, \phi_{2,R}$	ring rotations

ω	angular frequency, $2\pi f$, rad/sec

Subscripts:

c	associated with shell
j, m	denote jth and mth terms in power series and matrix elements
R	associated with ring
t	total
u, v, w	associated with displacements u, v, and w

Superscript:

T	transpose of a matrix

Dots over symbols denote partial differentiation with time t; for example, $\dot{u} = \frac{\partial u}{\partial t}$, $\ddot{u} = \frac{\partial^2 u}{\partial t^2}$.

Primes with symbol X indicate differentiation with respect to meridional coordinate s; for example, $X'_m = \frac{dX_m}{ds}$, $X''_m = \frac{d^2X_m}{ds^2}$.

A circumflex $\hat{}$ over a symbol denotes that the quantity is associated with local coordinate system of ring (see fig. 1(a)).

METHOD OF ANALYSIS

The analytical frequencies and mode shapes were obtained by use of the Rayleigh-Ritz procedure for the ring-stiffened, truncated conical shell shown in figure 1(a). In-plane and normal shell displacements u, v, and w are each assumed to be products of single-term circumferential modes and multiterm meridional modes. The circumferential modes are expressed by trigonometric functions and the meridional modes are given by general functions that may be chosen to satisfy particular displacement conditions at the ends of the shell. Here, power-series functions are used, with the series altered so as to satisfy displacement conditions for a clamped-free shell.

The ring is of arbitrary cross-sectional shape and is treated as a discrete element moving with the shell. Stiffness and mass properties are assumed to be concentrated at the ring location (i.e., in terms of $(EA)_R$, $(EI_S)_R$, etc.) with the ring mass concentrated at the ring center of gravity. Stiffener eccentricity effects due to rings attached inside or outside the shell wall are explicitly considered, as in reference 8, for reinforced cylindrical shells. An approximate frequency equation for the free ring is also derived in addition to the shell-ring frequency equation.

Strain-Displacement Relations

The basic strain-displacement relations used in the strain-energy expressions of the shell-ring combination are written in terms of the geometry and coordinate system of figure 1(a). The ring is assumed to be attached to the shell so that, in the manner of references 8 and 9, the displacements in the ring are compatible with those in the shell middle surface at the ring-shell junction.

Isotropic shell.- The following strain-displacement relations for the conical shell are based on reference 10:

$$\epsilon_{11} = \frac{\partial u}{\partial s} \tag{1a}$$

$$\epsilon_{22} = \frac{1}{r}\left(\frac{\partial v}{\partial \phi} + u \sin \delta + w \cos \delta\right) \tag{1b}$$

$$\epsilon_{12} = \frac{1}{2r}\left(r \frac{\partial v}{\partial s} + \frac{\partial u}{\partial \phi} - v \sin \delta\right) \tag{1c}$$

$$\kappa_{11} = - \frac{\partial^2 w}{\partial s^2} \tag{1d}$$

$$\kappa_{22} = \frac{1}{r^2}\left(\frac{\partial v}{\partial \phi} \cos \delta - \frac{\partial^2 w}{\partial \phi^2}\right) - \frac{\sin \delta}{r} \frac{\partial w}{\partial s} \tag{1e}$$

$$\bar{\kappa}_{12} = \frac{1}{r}\left(\frac{3}{4} \frac{\partial v}{\partial s} \cos \delta - \frac{\partial^2 w}{\partial s \, \partial \phi} + \frac{\sin \delta}{r} \frac{\partial w}{\partial \phi} - \frac{3v \cos \delta \sin \delta}{4r} - \frac{\cos \delta}{4r} \frac{\partial u}{\partial \phi}\right) \tag{1f}$$

where ϵ_{11}, ϵ_{22}, ϵ_{12} are associated with the shell membrane (or extensional) properties and κ_{11}, κ_{22}, $\bar{\kappa}_{12}$ with shell bending and torsion. The subscript 1 identifies the meridional direction and the subscript 2 denotes the circumferential direction.

Rings.- The ring strain-displacement relation may be written as

$$e_{22,R} = \epsilon_{22,R} + z\kappa_{22,R} - \hat{s}\left[\frac{1}{r_R^2}\left(\frac{\partial^2 u}{\partial \phi^2}\right)_R - \frac{\cos \delta}{r_R}\left(\frac{\partial w}{\partial s}\right)_R - z\left(\frac{\partial^3 w}{r^2 \, \partial \phi^2 \, \partial s}\right)_R\right] \tag{2}$$

where the first two terms represent the commonly used, or primary, extensional and bending properties of the ring, and the remaining terms represent secondary effects to be investigated. These effects are out-of-plane bending, cross-sectional asymmetry, and warping. These additional terms are derived in appendix A by the approach used in reference 9.

The effect of ring torsion is approximated by assuming that the torsional strain-displacement relation is given by $\bar{\kappa}_{12}$ (eq. (1f)) evaluated at $r = r_R$.

Strain Energies

Isotropic shell.- To be consistent with reference 10 and equations (1), the shell strain energy may be expressed by

$$U_c = \frac{E_c h}{2(1-\mu^2)} \int_{s_1}^{s_2} \int_0^{2\pi} \left[\epsilon_{11}^2 + 2\mu\epsilon_{11}\epsilon_{22} + \epsilon_{22}^2 + 2(1-\mu)\epsilon_{12}^2 \right] r \, d\phi \, ds$$

$$+ \frac{E_c h^3}{24(1-\mu^2)} \int_{s_1}^{s_2} \int_0^{2\pi} \left[\kappa_{11}^2 + 2\mu\kappa_{11}\kappa_{22} + \kappa_{22}^2 + 2(1-\mu)\bar{\kappa}_{12}^2 \right] r \, d\phi \, ds \qquad (3)$$

for a shell of constant thickness h, Young's modulus E_c, and Poisson's ratio μ. Substitution of equations (1) into equation (3) yields

$$U_c = \frac{E_c h}{2(1-\mu^2)} \int_{s_1}^{s_2} \int_0^{2\pi} \left[\left(\frac{\partial u}{\partial s} \right)^2 + 2 \frac{\mu}{r} \frac{\partial u}{\partial s} \left(\frac{\partial v}{\partial \phi} + u \sin\delta + w \cos\delta \right) + \frac{1}{r^2} \left(\frac{\partial v}{\partial \phi} + u \sin\delta + w \cos\delta \right)^2 \right.$$

$$\left. + \frac{1-\mu}{2r^2} \left(r \frac{\partial v}{\partial s} + \frac{\partial u}{\partial \phi} - v \sin\delta \right)^2 \right] r \, d\phi \, ds + \frac{E_c h^3}{24(1-\mu^2)} \int_{s_1}^{s_2} \int_0^{2\pi} \left\{ \left(\frac{\partial^2 w}{\partial s^2} \right)^2 \right.$$

$$- 2 \frac{\mu}{r} \frac{\partial^2 w}{\partial s^2} \left[\frac{1}{r} \left(\frac{\partial v}{\partial \phi} \cos\delta - \frac{\partial^2 w}{\partial \phi^2} \right) - \frac{\partial w}{\partial s} \sin\delta \right] + \frac{1}{r^2} \left[\frac{1}{r} \left(\frac{\partial v}{\partial \phi} \cos\delta - \frac{\partial^2 w}{\partial \phi^2} \right) - \frac{\partial w}{\partial s} \sin\delta \right]^2$$

$$\left. + \frac{2(1-\mu)}{r^2} \left(\frac{3}{4} \frac{\partial v}{\partial s} \cos\delta - \frac{\partial^2 w}{\partial s \, \partial \phi} - \frac{3v \cos\delta \sin\delta}{4r} + \frac{\sin\delta}{r} \frac{\partial w}{\partial \phi} - \frac{\cos\delta}{4r} \frac{\partial u}{\partial \phi} \right)^2 \right\} r \, d\phi \, ds \qquad (4)$$

Rings.- With the rings treated as discrete elements, the strain energy for M-rings is given by

$$U_R = \frac{1}{2} \sum_{k=1}^{M} \left[\int_0^{2\pi} \int_{A_R} E_R e_{22,R}^2 \, dA_R \, r_R \, d\phi + \int_0^{2\pi} (GJ)_R \bar{\kappa}_{12}^2 \, r_R \, d\phi \right]_k \qquad (5)$$

where each ring may be of a different material. If each ring is assumed to be uniform around its circumference, equation (2) and equation (1f) may be substituted into equation (5) to give

$$U_R = \frac{1}{2}\sum_{k=1}^{M}\frac{1}{r_{Rk}}\Bigg\{(EA)_R\int_0^{2\pi}\left(\frac{\partial v}{\partial\phi}+u\sin\delta+w\cos\delta\right)_R^2 d\phi$$

$$+2(EA)_R z_R\int_0^{2\pi}\left(\frac{\partial v}{\partial\phi}+u\sin\delta+w\cos\delta\right)_R\left[\frac{1}{r}\left(\frac{\partial v}{\partial\phi}\cos\delta-\frac{\partial^2 w}{\partial\phi^2}\right)-\frac{\partial w}{\partial s}\sin\delta\right]_R d\phi$$

$$+(EI_s)_R\int_0^{2\pi}\left[\frac{1}{r}\left(\frac{\partial v}{\partial\phi}\cos\delta-\frac{\partial^2 w}{\partial\phi^2}\right)-\frac{\partial w}{\partial s}\sin\delta\right]_R^2 d\phi+(GJ)_R\int_0^{2\pi}\left(\frac{3}{4}\frac{\partial v}{\partial s}\cos\delta\right.$$

$$\left.-\frac{\partial^2 w}{\partial s\,\partial\phi}-\frac{3v\cos\delta\sin\delta}{4r}+\frac{\sin\delta}{r}\frac{\partial w}{\partial\phi}-\frac{\cos\delta}{4r}\frac{\partial u}{\partial\phi}\right)_R^2 d\phi\Bigg\}_k+\Delta U_R \qquad (6)$$

where the terms within the summation contain the primary ring stiffness and eccentricity effects, and ΔU_R represents the contribution of the secondary stiffness and eccentricity terms as follows:

$$\Delta U_R = \frac{1}{2}\sum_{k=1}^{M}\frac{1}{r_{Rk}}\Bigg\{-2(EA)_R\hat{s}_R\int_0^{2\pi}\left(\frac{\partial v}{\partial\phi}+u\sin\delta+w\cos\delta\right)_R\left(\frac{\partial^2 u}{r\,\partial\phi^2}-\frac{\partial w}{\partial s}\cos\delta\right)_R d\phi$$

$$-2(EI_{sz})_R\int_0^{2\pi}\left[\frac{1}{r}\left(\frac{\partial v}{\partial\phi}\cos\delta-\frac{\partial^2 w}{\partial\phi^2}\right)-\frac{\partial w}{\partial s}\sin\delta\right]_R\left(\frac{\partial^2 u}{r\,\partial\phi^2}-\frac{\partial w}{\partial s}\cos\delta\right)_R d\phi$$

$$+2\frac{(EI_{sz})_R}{r_R}\int_0^{2\pi}\left(\frac{\partial v}{\partial\phi}+u\sin\delta+w\cos\delta\right)_R\left(\frac{\partial^3 w}{\partial\phi^2\,\partial s}\right)_R d\phi$$

$$+(EI_z)_R\int_0^{2\pi}\left(\frac{\partial^2 u}{r\,\partial\phi^2}-\frac{\partial w}{\partial s}\cos\delta\right)_R^2 d\phi+2\frac{(EI_1)_R}{r_R}\int_0^{2\pi}\left[\frac{1}{r}\left(\frac{\partial v}{\partial\phi}\cos\delta-\frac{\partial^2 w}{\partial\phi^2}\right)\right.$$

$$\left.-\frac{\partial w}{\partial s}\sin\delta\right]_R\left(\frac{\partial^3 w}{\partial\phi^2\,\partial s}\right)_R d\phi-2\frac{(EI_2)_R}{r_R}\int_0^{2\pi}\left(\frac{\partial^2 u}{r\,\partial\phi^2}-\frac{\partial w}{\partial s}\cos\delta\right)_R\left(\frac{\partial^3 w}{\partial\phi^2\,\partial s}\right)_R d\phi$$

$$+\frac{(E\Gamma)_R}{r_R^2}\int_0^{2\pi}\left(\frac{\partial^3 w}{\partial\phi^2\,\partial s}\right)_R^2 d\phi\Bigg\}_k \qquad (7)$$

The cross-sectional properties in equations (6) and (7) result from integration over the ring cross section in the double integral of equation (5) and are defined as follows:

$$\left.\begin{aligned}
&\int_{A_R} dA_R = A_R \qquad \int_{A_R} \hat{s}\, dA_R = A_R\hat{s}_R \qquad \int_{A_R} \hat{s}z^2\, dA_R = I_{1,R} \\
&\int_{A_R} z\, dA_R = A_R z_R \qquad \int_{A_R} \hat{s}z\, dA_R = I_{sz,R} \qquad \int_{A_R} (\hat{s})^2 z\, dA_R = I_{2,R} \\
&\int_{A_R} z^2\, dA_R = I_{s,R} \qquad \int_{A_R} (\hat{s})^2\, dA_R = I_{z,R} \qquad \int_{A_R} (\hat{s}z)^2\, dA_R = \Gamma_R
\end{aligned}\right\} \tag{8}$$

The properties in the left column of equations (8) identify the primary membrane and bending stiffnesses $(EA)_R$ and $(EI_s)_R$ and the primary eccentricity term z_R which locates the ring centroid inside or outside the shell wall. The properties in the middle and right columns of equations (8) identify the secondary stiffness and eccentricity terms, with $\hat{s}_R$ giving the meridional position of the ring centroid and $(EI_z)_R$, $(EI_{sz})_R$, and $(E\Gamma)_R$ being the out-of-plane bending stiffness, the product-of-inertia stiffness, and the ring warping stiffness, respectively. All these properties are computed with respect to the $\hat{s},\hat{z}$ axes shown in figure 1(a). The moments of inertia $I_{s,R}$ and $I_{z,R}$ may also be written as

$$I_{s,R} = I_{os,R} + A_R z_R^2 \tag{9a}$$

$$I_{z,R} = I_{oz,R} + A_R(\hat{s}_R)^2 \tag{9b}$$

where $I_{os,R}$ and $I_{oz,R}$ are moments of inertia of the ring about the centroidal axes parallel to the s-axis and z-axis, respectively.

It is noted here that the strain-displacement relations for the primary stiffnesses in equation (6) satisfy all the rigid-body modes of a conical shell, whereas the strain-displacement relations for the secondary stiffnesses in equation (7) satisfy only some of these modes, as is shown in appendix A. This and other features of the secondary stiffnesses are discussed further in the application of the analysis.

Kinetic Energies

Isotropic shell.- The kinetic energy of the isotropic shell (neglecting rotatory inertia) is given by

$$T_c = \frac{\rho_c h}{2} \int_{s_1}^{s_2} \int_0^{2\pi} (\dot{u}^2 + \dot{v}^2 + \dot{w}^2) r\, d\phi\, ds \tag{10}$$

where ρ_c is the mass density of the shell.

Rings.- With the rings treated as discrete elements, the kinetic energy for M-rings may be written as follows:

$$T_R = \frac{1}{2}\sum_{k=1}^{M}\left[\rho_R \int_0^{2\pi}\int_{A_R}\left(\dot{\bar{u}}_t^2 + \dot{\bar{v}}_t^2 + \dot{\bar{w}}_t^2\right)dA_R\, r_R\, d\phi\right]_k \tag{11}$$

where ρ_R is the mass density of the ring and the barred quantities denote total velocities at any point in the ring, which are given by

$$\left.\begin{aligned}
\dot{\bar{u}}_{t,R} &= \dot{u}_R + z\dot{\phi}_{1,R} \\
\dot{\bar{v}}_{t,R} &= \dot{v}_R + z\dot{\phi}_{2,R} - \frac{\hat{s}}{r_R}\left[\left(\frac{\partial \dot{u}}{\partial \phi}\right)_R + z\left(\frac{\partial \dot{\phi}_1}{\partial \phi}\right)_R\right] \\
\dot{\bar{w}}_{t,R} &= \dot{w}_R - \hat{s}\dot{\phi}_{1,R}
\end{aligned}\right\} \tag{12}$$

with

$$\dot{\phi}_{1,R} = \left(-\frac{\partial \dot{w}}{\partial s}\right)_R \tag{13a}$$

and

$$\dot{\phi}_{2,R} = \frac{1}{r_R}\left(\dot{v}\cos\delta - \frac{\partial \dot{w}}{\partial \phi}\right)_R \tag{13b}$$

Equations (12) are based on the displacements given by equations (A3).

Substitution of equations (12) and (13) into equation (11) and integration over the ring cross-sectional area leads to the following expression for the ring kinetic energy:

$$T_R = \frac{1}{2}\sum_{k=1}^{M}\left[\rho_R \int_0^{2\pi} A_R\left(\dot{u}_R^2 + \dot{v}_R^2 + \dot{w}_R^2\right) r_R\, d\phi\right]_k + \Delta T_R \tag{14}$$

where the primary mass effects are contained within the summation term, and ΔT_R representing the secondary rotatory, eccentricity, and warping inertia contributions is given by

$$\Delta T_R = \frac{1}{2}\sum_{k=1}^{M}\Bigg(\rho_R\int_0^{2\pi}\Bigg\{2A_R z_R\Bigg[-\dot{u}\,\frac{\partial\dot{w}}{\partial s}+\frac{\dot{v}}{r}\Big(\dot{v}\cos\delta-\frac{\partial\dot{w}}{\partial\phi}\Big)\Bigg]_R+2A_R\hat{s}_R\Big(\dot{w}\,\frac{\partial\dot{w}}{\partial s}-\frac{\dot{v}}{r}\,\frac{\partial\dot{u}}{\partial\phi}\Big)_R$$

$$+J_{e,R}\Big(\frac{\partial\dot{w}}{\partial s}\Big)_R^2+\frac{I_{s,R}}{r_R^2}\Big(\dot{v}\cos\delta-\frac{\partial\dot{w}}{\partial\phi}\Big)_R^2+\frac{I_{z,R}}{r_R^2}\Big(\frac{\partial\dot{u}}{\partial\phi}\Big)_R^2+2\,\frac{I_{sz,R}}{r_R}\Bigg[\dot{v}\,\frac{\partial^2\dot{w}}{\partial s\,\partial\phi}$$

$$-\frac{1}{r}\,\frac{\partial\dot{u}}{\partial\phi}\Big(\dot{v}\cos\delta-\frac{\partial\dot{w}}{\partial\phi}\Big)\Bigg]_R+2\,\frac{I_{1,R}}{r_R^2}\Big(\frac{\partial^2\dot{w}}{\partial s\,\partial\phi}\Big)_R\Big(\dot{v}\cos\delta-\frac{\partial\dot{w}}{\partial\phi}\Big)_R-2\,\frac{I_{2,R}}{r_R^2}\Big(\frac{\partial\dot{u}}{\partial\phi}\Big)_R\Big(\frac{\partial^2\dot{w}}{\partial s\,\partial\phi}\Big)_R$$

$$+\frac{\Gamma_R}{r_R^2}\Big(\frac{\partial^2\dot{w}}{\partial s\,\partial\phi}\Big)_R^2\Bigg\}r_R\,d\phi\Bigg)_k \tag{15}$$

The polar moment of inertia of the ring cross section is

$$J_{e,R}=\int_{A_R}\Big[z^2+(\hat{s})^2\Big]dA_R$$

Modal Functions

The in-plane and normal displacements u, v, and w are represented by

$$u(s,\phi,t)=\cos n\phi\sum_{m=P}^{Q}a_m(t)X_{mu}(s) \tag{16a}$$

$$v(s,\phi,t)=\sin n\phi\sum_{m=P}^{Q}b_m(t)X_{mv}(s) \tag{16b}$$

$$w(s,\phi,t)=\cos n\phi\sum_{m=P}^{Q}c_m(t)X_{mw}(s) \tag{16c}$$

The lower limit in each summation is determined by the functions chosen for the X_m's and the displacement conditions at the ends of the shell. In the present study, the meridional mode shapes were approximated by simple power-series functions, namely,

$$X_{mu}=X_{mv}=X_{mw}=\Big(\frac{s-s_1}{s_2-s_1}\Big)^m$$

with $m=1$ for the lower limit in u and v and $m=2$ for the lower limit in w so as to satisfy the displacement conditions

$$u = v = w = \frac{\partial w}{\partial s} = 0$$

at $s = s_1$ for a clamped-free shell. When $m = 0$ for the lower limits of all three displacements, these functions are applicable to a free-free conical shell.

General Form of Frequency Equation

As a result of substituting equations (16) into the expressions for the strain and kinetic energies of the shell and those of the ring and adding them together, the equations of motion may be obtained from the following relations in accordance with the Rayleigh-Ritz procedure with $a_j(t) = \bar{a}_j e^{i\omega t}$, and so forth, for simple harmonic motion of frequency ω:

$$\left.\begin{aligned}
\frac{\partial}{\partial \bar{a}_j}\left\{U_c(\bar{a}_j) + U_R(\bar{a}_j) - \omega^2\left[T_c(\bar{a}_j) + T_R(\bar{a}_j)\right]\right\} &= 0 \\
\frac{\partial}{\partial \bar{b}_j}\left\{U_c(\bar{b}_j) + U_R(\bar{b}_j) - \omega^2\left[T_c(\bar{b}_j) + T_R(\bar{b}_j)\right]\right\} &= 0 \\
\frac{\partial}{\partial \bar{c}_j}\left\{U_c(\bar{c}_j) + U_R(\bar{c}_j) - \omega^2\left[T_c(\bar{c}_j) + T_R(\bar{c}_j)\right]\right\} &= 0
\end{aligned}\right\} \tag{17}$$

In the present application, the maximum range of j was from 1 to 19. The operations indicated in equations (17) lead to the familiar algebraic eigenvalue form

$$\left[\begin{bmatrix} A & B & E \\ B^T & F & G \\ E^T & G^T & H \end{bmatrix}_c + \frac{1-\mu^2}{E_c h}\sum_{k=1}^{M}\begin{bmatrix} A & B & E \\ B^T & F & G \\ E^T & G^T & H \end{bmatrix}_R - \bar{\Delta}\left(\begin{bmatrix} \alpha & 0 & 0 \\ 0 & \beta & 0 \\ 0 & 0 & \gamma \end{bmatrix}_c + \sum_{k=1}^{M}\begin{bmatrix} \alpha & \alpha\beta & \alpha\gamma \\ (\alpha\beta)^T & \beta & \beta\gamma \\ (\alpha\gamma)^T & (\beta\gamma)^T & \gamma \end{bmatrix}_R\right)\right]\begin{Bmatrix} \bar{a} \\ \bar{b} \\ \bar{c} \end{Bmatrix} = \begin{Bmatrix} 0 \\ 0 \\ 0 \end{Bmatrix} \tag{18}$$

where the eigenvalue $\bar{\Delta}$ is equal to $\dfrac{\rho_c r_0^2 \omega^2 (1-\mu^2)}{E_c}$ with r_0 arbitrarily chosen as the average radius of the shell $\dfrac{r_1 + r_2}{2}$ in terms of the end radii r_1 and r_2 (fig. 1(a)). The letters inside the square matrices of equation (18) represent submatrices whose

elements are given in appendix B. The letters inside the column matrix represent submatrices of the amplitude coefficients introduced into equations (17).

The solution of equation (18) was programed in double precision arithmetic (29 significant figures) for the Control Data 6600 computer system, with eigenvalues and eigenvectors obtained by use of the threshold Jacobi method described in reference 11, for example.

Ring Frequency Equation

An approximate frequency equation of a conically oriented free ring was derived on the basis of the ring strain and kinetic energies from equations (6), (7), (14), and (15). Four degrees of freedom were assumed: three displacements u_R, v_R, w_R of the free-ring elastic axis and twist about the elastic axis β_R, which replaces $\left(-\frac{\partial w}{\partial s}\right)_R$ in the ring strain and kinetic energies since the ring is no longer constrained to move with the shell. The term $(\partial v/\partial s)_R$ in equation (6) is omitted. By following essentially the same procedure used for the derivation of equation (18), these variables were represented by

$$\left.\begin{aligned} u_R(\phi,t) &= \bar{a}_{n,R} e^{i\omega t} \cos n\phi \\ v_R(\phi,t) &= \bar{b}_{n,R} e^{i\omega t} \sin n\phi \\ w_R(\phi,t) &= \bar{c}_{n,R} e^{i\omega t} \cos n\phi \\ \beta_R(\phi,t) &= \bar{d}_{n,R} e^{i\omega t} \cos n\phi \end{aligned}\right\} \tag{19}$$

(where $\bar{a}_{n,R}$, $\bar{b}_{n,R}$, $\bar{c}_{n,R}$, and $\bar{d}_{n,R}$ are amplitude coefficients for the ring) and the equations of motion were obtained from the ring portions of equations (17). The resulting approximate frequency equation may be written in the general form

$$\left[[K] - \bar{\Delta}_R[M]\right] \begin{Bmatrix} \bar{a}_{n,R} \\ \cdot \\ \cdot \\ \cdot \\ \bar{d}_{n,R} \end{Bmatrix} = \begin{Bmatrix} 0 \\ \cdot \\ \cdot \\ \cdot \\ 0 \end{Bmatrix} \tag{20}$$

where $\bar{\Delta}_R = \rho_R r_R^2 A_R \omega^2$. Elements of the K and M 4×4 matrices, together with pertinent details of the derivation, are given in appendix C.

APPLICATION OF ANALYSIS

The analysis described in the preceding sections was applied to a ring-stiffened, isotropic, conical shell with a 60° semivertex angle. Vibration-test results for this configuration were obtained in an unpublished study by Eugene C. Naumann, John S. Mixson, and Earl C. Steeves. Comparisons are made between analytical and experimental frequencies and mode shapes of the clamped-free shell with a ring of rectangular cross section and with one and two ring stiffeners of Z-shaped cross section. The data needed for the calculations are listed in table I along with the properties defined in equations (8) for the ring cross-sectional geometries specified in figure 1(b). The rings were attached to the shell by rivets and ~~spot welds~~ bonding between the rivets. Both shell and rings were made of the same material (6061 aluminum alloy) so that $E_c = E_R$ and $\rho_c = \rho_R$. Frequencies obtained from equation (20) are compared with experimental frequencies for the conically oriented free Z-rings.

Comparison of Analytical and Experimental Results

Frequencies and mode shapes obtained by application of equations (18) and (20) are compared with experimental frequencies and mode shapes in tables II to V and figures 2 to 7. The existence of two (or more) experimental frequencies for the same mode shape is associated with the well-known phenomenon of dual resonances characteristic of rotationally symmetric structures. The distributions of the normal displacement w along the meridian are plotted in figures 3, 5, and 7. Comparisons between experiment and theory are made first for the shell-ring combination on the basis of the primary ring stiffness and mass terms in the analysis. Next, analytical and experimental free-ring frequencies are compared with each other and with analytical shell-ring frequencies based on the primary terms. Finally, the effects of ring secondary stiffnesses and inertias in the analysis are considered.

Shell with ring at base attachment.- Analytical and experimental frequencies and mode shapes of the conical shell without the Z-rings are presented in table II and figures 2 and 3. The experimental shell frequencies and mode shapes from the aforementioned unpublished study were measured for two different end-clamping conditions, one with a 3-inch small-end radius and the other with a 4-inch radius. Comparisons between analysis and experiment in this paper apply to the 3-inch (76.2 mm) model, in which the clamped end was reinforced by a thick circular block with a ring of rectangular cross section to which the shell was mounted, as shown schematically in figures 1(b) and 2. This "base" ring was assumed to move with the shell and was treated in the analysis as a discrete element, just as the Z-rings were.

Generally, excellent agreement between theory and experiment was obtained over the n-range from 0 to 15. Table II shows the nature of the analytical convergence; the frequencies are satisfactorily converged with 12 power-series terms approximating the meridional mode shapes of the w-displacement and 13 terms each approximating the u- and v-meridional mode shapes. It is also evident that frequencies for high n-values, above the n-value for minimum frequency, converged with fewer meridional terms than frequencies for lower n-values.

Primary stiffness effects of one Z-ring.- Analytical and experimental frequencies and mode shapes of the shell stiffened with the base ring and one ring of Z-shaped cross section at the large free end of the shell are presented in table III and figures 4(a) and 5. Converged analytical frequencies based on the primary ring terms are in excellent overall agreement with experimental frequencies for $m = 1$, and the agreement is generally good for $m = 2$. In figure 5 good agreement is shown between experimental and analytical mode shapes based on the primary ring terms, except in the vicinity of the ring location. Here, the analysis predicts a localized effect that was not observed in the corresponding experimental mode shapes (see $m = 1$ and $n =$ [illegible] and [illegible] in fig. 5(a); $m = 2$ and $n = 5$, 6, and 8 in fig. 5(b)).

The humps in the frequency variations of figure 4 and the character of the mode shapes in figure 5 are similar to those obtained by Newton in reference 6 for tubular rings on a shell with a cone angle of 15.9°. Of possible further interest is the close agreement in figure 4(b) of the trends in the frequencies of the conically oriented free ring and the ring-shell frequencies in the regions of the curves where ring effects predominated. The free-ring frequencies calculated by use of equation (20) are given in table V and are seen to be in fair agreement with experimental free-ring frequencies. The letters denoting the largest eigenvectors in the analytical frequencies given in table V indicate the predominance of one of the four motions involved. From table V(a), it is evident that the w-motion predominated for $n = 2$ and 3 and the u-motion predominated for $n = 4$ to 10 of the first family of modes for the large ring. For the second modal family, the rotation β_R predominated for $n = 6$ to 10, u_R for $n = 2$ and 3, and w_R for $n = 4$ and 5.

Except for $m = 2$ and $n = 6$, table III shows satisfactory convergence in frequencies with 16 w-terms and 17 u- and v-terms each. The table and figure 4(a) also indicate convergence with four fewer terms for $m = 1$ and $n = 0$ to 2, 6 to 18 and for $m = 2$ and $n = 9$ to 18 which are ranges where the shell effects predominated. The need for the four additional terms is clearly evident for $m = 1$ and $n = 3$ to 5 and for $m = 2$ and $n = 5$ to 8 in which the Z-ring effect was predominant.

Primary stiffness effects of two Z-rings.- Analytical and experimental frequencies and mode shapes are presented in table IV and figures 6 and 7 for the effects of an

additional Z-ring halfway along the meridian between the large and small ends of the shell, as shown in the sketch of figure 6(a). As for the model with one Z-ring at the free end of the shell, converged analytical frequencies based on the primary ring terms are in generally good agreement with experimental frequencies, the agreement being better for $m = 1$ than for $m = 2$ as figure 6(a) shows. However, agreement between theory and experiment is not as good for the two Z-ring model as for the one Z-ring model of figures 4 and 5. Figure 7(a) shows at least fair agreement between experimental and analytical mode shapes, even in the vicinity of the intermediate ring. The agreement near the large end ring is about the same as it was for the single Z-ring model.

Table IV indicates that 17 w-terms and 18 u- and v-terms were adequate to insure convergence of most of the analytical frequencies for the two Z-ring shell to the degree obtained for the single Z-ring shell. However, there were more modes requiring more power-series terms than for the single Z-ring model, and these modes were not confined to the ring-dominant regions of the curves as they were in the one Z-ring model. For example, with 18 w-terms and 19 u- and v-terms, the frequencies for $m = 2$ and $n = 2, 3, 4, 18, 19,$ and 22 were reduced significantly from the frequencies obtained with 17 w-terms and 18 u- and v-terms. Obtaining converged results for these modes by including still more power-series functions could not be accomplished because any additional terms would have caused enough numerical error in the solution of equation (18) to result in negative eigenvalues.

The effects of two Z-rings differ from those for one Z-ring by the existence of three minimum frequencies (fig. 6) instead of two as for the single Z-ring model (fig. 4). Figure 6(b) shows good agreement in the trends of both sets of free-ring frequencies with ring-shell frequencies in the ring-dominant regions of the curves. Equation (20) predicts the experimental frequencies of the small, conically oriented, free Z-ring about as well as it does for the large free Z-ring, although the discrepancy between theory and experiment becomes larger with increasing n-value. Table V(b) indicates a predominance in w_R for $n = 2$ and 3 and in u_R for $n = 4$ to 7 of the first family of free-ring modes. For the second family, u_R predominates for $n = 2$ and 3, w_R for $n = 4$, and β_R for $n = 5$ to 7.

Effects of ring secondary stiffnesses and inertias.- Inclusion of secondary stiffness and inertia terms (eqs. (7) and (15)) of the base ring resulted in increases in analytical frequencies of 7 percent for $m = 1$ and $n = 2$ and $3\frac{1}{2}$ percent for $m = 1$ and $n = 3$. (See table II.) Other frequencies within the n-range covered were negligibly affected by these additional terms. Meridional mode shapes shown in figure 3 were also negligibly different from those based only on the primary terms (eqs. (6) and (14)).

The effects of including secondary stiffnesses and inertias of the Z-rings are shown for the shell-ring frequencies in figures 4(a), 4(c), 6(a), and 6(c). The largest effects

occurred for modes in which the ring influence was the largest. For these modes, frequencies were reduced by as much as 43 percent (e.g., $m = 2$ and $n = 6$ in fig. 4(c)). Secondary inertias accounted for at least one-half of these frequency reductions which are considerably larger than those reported in the literature for stiffened cylindrical shells. The fact that these effects are in sharp contrast to the negligible effects obtained by McElman in reference 9 may be due largely to the conical orientation of the stiffeners and, to a smaller extent, to the Z-shaped stiffener cross section. Thin-wall rectangular and hat-shaped cross sections were considered in reference 9, and secondary inertias were not included therein. From figures 4(a) and 6(a), it is evident that inclusion of the secondary stiffnesses and inertias improved agreement between theory and experiment for some modes and not for others. For example, the agreement was improved for $m = 1$ and $n = 3$ in figure 4(a) and for $m = 1$ and $n = 3$ and for $m = 2$ and $n = 7$ in figure 6(a), but the agreement was made worse for $m = 1$ and $n = 8$ to 18 in figure 6(a).

Figures 5 and 7 indicate that the effects on analytical mode shapes of including secondary stiffness and inertia Z-ring terms were also largest for the ring-dominant modes. For the shell-dominant modes, these additional terms had a negligible effect on the mode shapes of the single Z-ring model and a small effect on those of the two Z-ring model. Large localized mode-shape variations close to the ring at the free end were obtained for the secondary terms as for the primary terms, but no consistent secondary effects were discernible in this region.

Limitations of the Analysis

Although the foregoing results indicate the adequacy of this type of modal analysis for prediction of the vibration modes of a locally reinforced conical shell, certain limitations encountered in the application of the analysis merit comment.

One such limitation is the number of functions that can be used to approximate the meridional mode shapes of the u-, v-, and w-displacements. More power-series functions are needed to obtain converged solutions as the number of discretely treated stiffeners increases, but the number of functions is limited by the accuracy obtainable in the solution of large-order eigenvalue equations of the form of equation (18). In the present study, no more than 19 simple power-series functions could be used to approximate each meridional displacement component for the two Z-ring model without causing enough loss of accuracy to result in negative eigenvalues. This loss of accuracy was due to the spread in magnitude between the highest and lowest eigenvalues of the mass-inertia matrix in excess of the double precision capabilities of the computer. Obtaining these eigenvalues is an essential step in the execution of the threshold Jacobi method, which, as previously noted, was used in this investigation.

Another limitation of the analysis is the failure of the strain-displacement relations for the secondary stiffnesses in equation (7) to satisfy all the rigid-body modes of the ring-stiffened conical shell or the conically oriented free ring. Consequently, the lowest free-free ring-shell or free-ring frequencies were not all zero for $n = 0$ and 1 as they should have been to correspond to rigid-body translations and rotations. This is evident in table V for the free-ring analytical frequencies and can also be shown for the frequencies of the free-free ring-stiffened shell. The effect of this limitation on the free-ring analytical frequencies for $n \geq 2$ could not be fully evaluated because both primary and secondary stiffness terms were needed to obtain meaningful frequencies from the solution of equation (20). (Secondary inertia effects are seen to be negligible.) These frequencies are therefore considered to be approximate at best, although they are in fair agreement with the experimental frequencies over the n-range covered. Comparisons (not included herein) of analytical shell-ring frequencies of the free-free base-ring configuration with and without secondary stiffnesses indicated frequency differences of over 40 percent for $n = 2$ in the second family of free-free modes ($m = 1$), with the differences diminishing to less than 1/2 percent at $n = 4$ and 5. Since, as previously noted, the strain-displacement relations associated with only the primary stiffnesses in equation (6) do satisfy all rigid-body translations and rotations, the four lowest free-free shell-ring frequencies for $m = 0$ and $n = 0$ and 1 and for $m = 1$ and $n = 0$ and 1 are zero for this approximation. The consequences of this limitation on the analytical clamped-free shell-ring vibration modes of the present study are not fully understood, but they are believed to be of less importance than they are for the free-free vibration modes.

CONCLUDING REMARKS

A Rayleigh-Ritz vibration analysis is described and applied to a wide-angle, isotropic, ring-stiffened conical shell for which experimental frequencies and mode shapes are available for comparison. Power-series functions are employed to approximate meridional mode shape components of the in-plane and normal displacements, and these series satisfy displacement boundary conditions for a conical-shell frustum clamped at the small end and free at the large end. Rings are treated as discrete elements of arbitrary cross section, and in the present study strong effects on the shell-ring vibration modes are shown for rings of Z-shaped cross section.

Good agreement between analytical and experimental frequencies and mode shapes was obtained for a shell with reinforced end clamping involving a base ring of rectangular cross section. Analytical results were converged with 12 power-series modal functions approximating the normal (or w) displacement component for the shell without Z-rings, 16 w-terms for the shell with a Z-ring attached at the free end, and with 17 w-terms for

the shell with two Z-rings. The agreement between analysis and experiment was best for the shell without Z-rings and was better for the shell with one Z-ring than for the shell with two Z-rings. The agreement was also better for circumferential modes where shell effects predominated than for these modes where ring effects predominated. Although the need for more power-series terms was indicated in order to converge some modes of the two Z-ring model, no more than 19 power-series functions could be used in the present analysis to obtain accurate results and possibly to improve agreement with experiment.

The results of this study also show that for this type of configuration significant effects and some improved agreement with experiment can be obtained by introducing into the analysis secondary terms to account for out-of-plane bending stiffness, stiffener asymmetry, warping, meridional eccentricity, and rotatory inertia. Inclusion of these secondary stiffnesses and inertias of the rectangular-shaped base ring produced generally negligible effects for the model without Z-rings. However, for the model with Z-rings, the effects on frequencies and mode shapes were large, with a change in frequency of over 40 percent occurring for some of the ring-dominant modes. For the shell-dominant modes, the secondary effects were negligible for the single Z-ring model and caused only a small change in frequency for the two Z-ring model.

Langley Research Center,
National Aeronautics and Space Administration,
Langley Station, Hampton, Va., November 24, 1969.

APPENDIX A

ESSENTIAL FEATURES IN THE DERIVATION OF STIFFNESSES IN A RING ATTACHED TO A CONICAL SHELL

This appendix presents the essential features of the derivation of the circumferential strain-displacement relation, equation (2) of the main text, and indicates how this relation is utilized to obtain the ring strain energies in equations (6) and (7). The derivation is the same as the one developed in reference 9 for doubly curved shells and is applied herein to a ring made up of thin cross-sectional members and mounted on a conical shell.

By following the procedure in chapter VII of reference 9, the total displacements in the ring in its local coordinate system (fig. 1(a)) may be written as

$$\left.\begin{aligned} \bar{u}_t(\hat{s},\hat{\phi},\hat{z}) &= \bar{u}(\hat{\phi},\hat{z}) \\ \bar{v}_t(\hat{s},\hat{\phi},\hat{z}) &= \bar{v}(\hat{\phi},\hat{z}) - \hat{s}\,\frac{\partial \bar{u}(\hat{\phi},\hat{z})}{r_R\,\partial\hat{\phi}} \\ \bar{w}_t(\hat{s},\hat{\phi},\hat{z}) &= \bar{w}(\hat{\phi},\hat{z}) - \hat{s}\,\frac{\partial \bar{u}(\hat{\phi},\hat{z})}{\partial\hat{z}} \end{aligned}\right\} \tag{A1}$$

where $\bar{u}$, $\bar{v}$, and $\bar{w}$ are displacements of the ring in the $\hat{\phi}$-$\hat{z}$ plane. (The subscript t in eqs. (A1), (A2), and (A3) denotes total displacement.) The relations in equations (A1) are based on the assumptions that the displacements are linear through the ring in the meridional direction and that transverse shear in this direction is neglected (i.e., $\bar{\gamma}\hat{s}\hat{\phi} = \bar{\gamma}\hat{s}\hat{z} = 0$ as in ref. 9). The displacements of equations (A1) must be compatible with those in the shell at the ring location, and this requirement is expressed by

$$\left.\begin{aligned} \bar{u}(\hat{\phi},\hat{z}) &= u_t(s_R,\phi,z) = u(s_R,\phi) + z\phi_{1,R} \\ \bar{v}(\hat{\phi},\hat{z}) &= v_t(s_R,\phi,z) = v(s_R,\phi) + z\phi_{2,R} \\ \bar{w}(\hat{\phi},\hat{z}) &= w_t(s_R,\phi,z) = w(s_R,\phi) \end{aligned}\right\} \tag{A2}$$

where $\phi_{1,R}$ and $\phi_{2,R}$ are rotations in the $\hat{s}$-$\hat{z}$ and ϕ-$\hat{z}$ planes, respectively, at the ring-shell interface and are given by

$$\phi_{1,R} = \left(-\frac{\partial w}{\partial s}\right)_R$$

and

$$\phi_{2,R} = \frac{1}{r_R}\left(v \cos \delta - \frac{\partial w}{\partial \phi}\right)_R$$

The expressions at the extreme right of equations (A2) are the total displacements in the shell at the ring location. They are assumed to be linear through the shell in the Z-direction, with $u(s_R,\phi)$, $v(s_R,\phi)$, and $w(s_R,\phi)$ being the displacements of the shell middle surface.

Substitution of equations (A2) into equations (A1) gives the following expressions for the ring displacements:

$$\left.\begin{aligned} \bar{u}_t &= u_R + z\phi_{1,R} \\ \bar{v}_t &= v_R + z\phi_{2,R} - \frac{\hat{s}}{r_R}\left(\frac{\partial u_R}{\partial \phi} + z\,\frac{\partial \phi_{1,R}}{\partial \phi}\right) \\ \bar{w}_t &= w_R - \hat{s}\phi_{1,R} \end{aligned}\right\} \tag{A3}$$

where

$$u_R = u(s_R,\phi)$$

$$v_R = v(s_R,\phi)$$

$$w_R = w(s_R,\phi)$$

$$\frac{\partial u_R}{\partial \phi} = \left.\frac{\partial u(s,\phi)}{\partial \phi}\right|_{s=s_R}$$

and

$$\frac{\partial \phi_{1,R}}{\partial \phi} = \left.\frac{\partial \phi_1(s,\phi)}{\partial \phi}\right|_{s=s_R}$$

The strain-displacement relations for the shell at the ring location may be written as follows:

$$\epsilon_{11,R} = 0 \tag{A4a}$$

$$\epsilon_{22,R} = \frac{1}{r_R}\left(\frac{\partial \bar{v}_t}{\partial \phi} + \bar{u}_t \sin \delta + \bar{w}_t \cos \delta\right) \tag{A4b}$$

APPENDIX A

Substitution of equations (A3) into equation (A4b) gives

$$e_{22,R} = \frac{1}{r_R}\left[\frac{\partial v_R}{\partial \phi} + u_R \sin\delta + w_R \cos\delta + z\left(\frac{\partial \phi_{2,R}}{\partial \phi} + \phi_{1,R}\sin\delta\right)\right.$$
$$\left. - \hat{s}\left(\frac{\partial^2 u_R}{r_R\,\partial\phi^2} + \phi_{1,R}\cos\delta + z\,\frac{\partial^2 \phi_{2,R}}{r_R\,\partial\phi^2}\right)\right] \qquad \text{(A5)}$$

Equation (A5) may also be written in the form of equation (2) in the main body of the report.

In the substitution of equation (2) and equation (1f) into equation (5) to yield equations (6) and (7), all the rigid-body modes listed in the following table are satisfied for the strain-displacement relations associated with the primary stiffnesses in equation (6):

Description	u	v	w
Axial displacement	$\cos\delta$	0	$-\sin\delta$
Roll about cone axis	0	r	0
Sidewise translation	$\cos\phi\sin\delta$	$-\sin\phi$	$\cos\phi\cos\delta$
Rotation about apex	0	$-s\cos\delta\sin\phi$	$s\cos\phi$

However, in equation (7), the strain-displacement relations $\left(\frac{\partial^2 u}{r\,\partial\phi^2} - \frac{\partial w}{\partial s}\cos\delta\right)_R$ and $\left(\frac{\partial^3 w}{\partial\phi^2\,\partial s}\right)_R$ satisfy only the rigid-body axial displacement and roll displacement about the cone axis but not the rigid-body side translation of the cone or "side" rotation of the cone about its apex. It may also be noted that the strain-displacement relations in references 8 and 9 do not satisfy all the rigid-body modes of a cylindrical shell, which may be obtained from those in the foregoing table with $\delta = 0$, s replaced by an axial coordinate x, and $u = -r\cos\phi$ for rotation about the end of the shell.

APPENDIX B

MATRIX ELEMENTS OF SHELL-RING FREQUENCY EQUATION

This appendix lists the matrix elements of equation (18). Included also are evaluated forms of the integrals and ring displacement components based on the power-series function

$$X_{mu} = X_{mv} = X_{mw} = \left(\frac{s - s_1}{s_2 - s_1}\right)^m$$

where, in general, $m = 0, 1, 2, \ldots$.

Shell Matrix Elements

The shell matrices in equation (18) are identified by the subscript c, and their elements are as follows:

$$A_{jm,c} = \sin\delta \int_{s_1}^{s_2} X'_{ju}X'_{mu}\, s\, ds + \mu \sin\delta \int_{s_1}^{s_2} \left(X_{ju}X'_{mu} + X'_{ju}X_{mu}\right) ds$$

$$+ \sin\delta\left(1 + \frac{n^2}{\sin^2\delta}\frac{1 - \mu}{2}\right)\int_{s_1}^{s_2} X_{ju}X_{mu}\frac{ds}{s} + \frac{n^2\cot^2\delta}{\sin\delta}\frac{h^2(1 - \mu)}{96}\int_{s_1}^{s_2} X_{ju}X_{mu}\frac{ds}{s^3} \tag{B1}$$

$$B_{jm,c} = n\left[\mu\int_{s_1}^{s_2} X'_{ju}\, X_{mv}\, ds + \int_{s_1}^{s_2} X_{ju}X_{mv}\frac{ds}{s} - \frac{1 - \mu}{2}\int_{s_1}^{s_2} X_{ju}\left(sX'_{mv} - X_{mv}\right)\frac{ds}{s}\right.$$

$$\left. + \left(\cot^2\delta\right)\frac{h^2(1 - \mu)}{32}\int_{s_1}^{s_2} X_{ju}\left(X'_{mv} - \frac{X_{mv}}{s}\right)\frac{ds}{s^2}\right] \tag{B2}$$

$$E_{jm,c} = \cos\delta\left[\mu\int_{s_1}^{s_2} X'_{ju}X_{mw}\, ds + \int_{s_1}^{s_2} X_{ju}X_{mw}\frac{ds}{s}\right.$$

$$\left. + \frac{n^2}{\sin^2\delta}\frac{h^2(1 - \mu)}{24}\int_{s_1}^{s_2} X_{ju}\left(X'_{mw} - \frac{X_{mw}}{s}\right)\frac{ds}{s^2}\right] \tag{B3}$$

APPENDIX B

$$F_{jm,c} = \frac{n^2}{\sin\delta}\int_{s_1}^{s_2} X_{jv}X_{mv}\frac{ds}{s} + (\sin\delta)\left(\frac{1-\mu}{2}\right)\int_{s_1}^{s_2}\left(sX'_{jv} - X_{jv}\right)\left(sX'_{mv} - X_{mv}\right)\frac{ds}{s}$$

$$+ \frac{n^2\cot^2\delta}{\sin\delta}\frac{h^2}{12}\int_{s_1}^{s_2} X_{jv}X_{mv}\frac{ds}{s^3} + (\cot\delta\cos\delta)\frac{3h^2(1-\mu)}{32}\int_{s_1}^{s_2}\left(X'_{jv} - \frac{X_{jv}}{s}\right)\left(X'_{mv} - \frac{X_{mv}}{s}\right)\frac{ds}{s} \qquad \text{(B4)}$$

$$G_{jm,c} = n\cot\delta\left[\int_{s_1}^{s_2} X_{jv}X_{mw}\frac{ds}{s} - \mu\frac{h^2}{12}\int_{s_1}^{s_2} X_{jv}X''_{mw}\frac{ds}{s}\right.$$

$$\left. + \csc\delta\frac{h^2}{12}\int_{s_1}^{s_2} X_{jv}\left(\frac{n^2X_{mw}}{s\sin\delta} - X'_{mw}\sin\delta\right)\frac{ds}{s^2} + \frac{h^2(1-\mu)}{8}\int_{s_1}^{s_2}\left(X'_{jv} - \frac{X_{jv}}{s}\right)\left(X'_{mw} - \frac{X_{mw}}{s}\right)\frac{ds}{s}\right] \qquad \text{(B5)}$$

$$H_{jm,c} = \cot\delta\cos\delta\int_{s_1}^{s_2} X_{jw}X_{mw}\frac{ds}{s} + \frac{h^2}{12}\left[\sin\delta\int_{s_1}^{s_2} X''_{jw}X''_{mw}s\,ds\right.$$

$$- \mu\int_{s_1}^{s_2}\left(\frac{n^2X_{jw}}{s\sin\delta} - X'_{jw}\sin\delta\right)X''_{mw}\,ds - \mu\int_{s_1}^{s_2} X''_{jw}\left(\frac{n^2X_{mw}}{s\sin\delta} - X'_{mw}\sin\delta\right)ds$$

$$+ \csc\delta\int_{s_1}^{s_2}\left(\frac{n^2X_{jw}}{s\sin\delta} - X'_{jw}\sin\delta\right)\left(\frac{n^2X_{mw}}{s\sin\delta} - X'_{mw}\sin\delta\right)\frac{ds}{s}$$

$$\left. + 2n^2(1-\mu)\csc\delta\int_{s_1}^{s_2}\left(X'_{jw} - \frac{X_{jw}}{s}\right)\left(X'_{mw} - \frac{X_{mw}}{s}\right)\frac{ds}{s}\right] \qquad \text{(B6)}$$

$$\left.\begin{aligned}
\alpha_{jm,c} &= \frac{\sin\delta}{r_0^2}\int_{s_1}^{s_2} X_{ju}X_{mu}s\,ds \\
\beta_{jm,c} &= \frac{\sin\delta}{r_0^2}\int_{s_1}^{s_2} X_{jv}X_{mv}s\,ds \\
\gamma_{jm,c} &= \frac{\sin\delta}{r_0^2}\int_{s_1}^{s_2} X_{jw}X_{mw}s\,ds
\end{aligned}\right\} \qquad \text{(B7)}$$

where r has been replaced by $s\sin\delta$, and primes with the symbol X denote differentiation with respect to s.

APPENDIX B

Ring Matrix Elements

The ring matrices in equation (18) are identified by the subscript R, and their elements are as follows:

$$A_{jm,R} = \frac{1}{r_R}\left[(EA)_R \sin^2\delta + (GJ)_R\left(\frac{n\cos\delta}{4r_R}\right)^2\right]X_{ju,R}X_{mu,R} + \Delta A_{jm,R} \tag{B8}$$

$$B_{jm,R} = \frac{n}{r_R}X_{ju,R}\left[(EA)_R \sin\delta\left(1 + \frac{z_R}{r_R}\cos\delta\right)X_{mv,R} + \frac{3(GJ)_R}{16r_R}\cos^2\delta\left(X'_{mv,R} - \frac{X_{mv,R}\sin\delta}{r_R}\right)\right] + \Delta B_{jm,R} \tag{B9}$$

$$E_{jm,R} = \frac{\sin\delta}{r_R}X_{ju,R}\left[(EA)_R X_{mw,R}\cos\delta + (EA)_R z_R\left(\frac{n^2X_{mw,R}}{r_R} - X'_{mw,R}\sin\delta\right)\right.$$
$$\left. + (GJ)_R\frac{n^2\cot\delta}{4r_R}\left(X'_{mw,R} - \frac{X_{mw,R}\sin\delta}{r_R}\right)\right] + \Delta E_{jm,R} \tag{B10}$$

$$F_{jm,R} = \frac{1}{r_R}\left[n^2(EA)_R\left(1 + 2\frac{z_R}{r_R}\cos\delta\right)X_{jv,R}X_{mv,R} + (EI_S)_R\left(\frac{n\cos\delta}{r_R}\right)^2 X_{jv,R}X_{mv,R}\right.$$
$$\left. + \frac{9}{16}(GJ)_R\cos^2\delta\left(X'_{jv,R} - \frac{X_{jv,R}\sin\delta}{r_R}\right)\left(X'_{mv,R} - \frac{X_{mv,R}\sin\delta}{r_R}\right)\right] \tag{B11}$$

$$G_{jm,R} = \frac{n}{r_R}\left[(EA)_R\cos\delta\left(1 + \frac{z_R}{r_R}\cos\delta\right)X_{jv,R}X_{mw,R} + (EA)_R X_{jv,R}z_R\left(\frac{n^2X_{mw,R}}{r_R} - X'_{mw,R}\sin\delta\right)\right.$$
$$+ \frac{(EI_S)_R}{r_R}X_{jv,R}\cos\delta\left(\frac{n^2X_{mw,R}}{r_R} - X'_{mw,R}\sin\delta\right)$$
$$\left. + \frac{3(GT)_R}{4}\cos\delta\left(X'_{jv,R} - \frac{X_{jv,R}\sin\delta}{r_R}\right)\left(X'_{mw,R} - \frac{X_{mw,R}\sin\delta}{r_R}\right)\right] + \Delta G_{jm,R} \tag{B12}$$

$$H_{jm,R} = \frac{1}{r_R}\left[(EA)_R X_{jw,R}X_{mw,R}\cos^2\delta + 2n^2(EA)_R\frac{z_R}{r_R}X_{jw,R}X_{mw,R}\cos\delta\right.$$
$$- (EA)_R z_R\sin\delta\cos\delta\left(X_{jw,R}X'_{mw,R} + X'_{jw,R}X_{mw,R}\right)$$
$$+ (EI_S)_R\left(\frac{n^2X_{jw,R}}{r_R} - X'_{jw,R}\sin\delta\right)\left(\frac{n^2X_{mw,R}}{r_R} - X'_{mw,R}\sin\delta\right)$$
$$\left. + n^2(GJ)_R\left(X'_{jw,R} - \frac{X_{jw,R}\sin\delta}{r_R}\right)\left(X'_{mw,R} - \frac{X_{mw,R}\sin\delta}{r_R}\right)\right] + \Delta H_{jm,R} \tag{B13}$$

APPENDIX B

$$\alpha_{jm,R} = \frac{\rho_R r_R}{r_0^2 \rho_c h} A_R X_{ju,R} X_{mu,R} + \Delta\alpha_{jm,R} \tag{B14}$$

$$(\alpha\beta)_{jm,R} = \frac{\rho_R r_R}{r_0^2 \rho_c h} n \left(A_R \frac{\hat{s}_R}{r_R} + \frac{I_{sz,R}}{r_R^2} \cos\delta \right) X_{ju,R} X_{mv,R} \tag{B15}$$

$$(\alpha\gamma)_{jm,R} = \frac{\rho_R r_R}{r_0^2 \rho_c h} \left[-\left(A_R z_R + n^2 \frac{I_{2,R}}{r_R^2} \right) X_{ju,R} X'_{mw,R} + n^2 \frac{I_{sz,R}}{r_R^2} X_{ju,R} X_{mw,R} \right] \tag{B16}$$

$$\beta_{jm,R} = \frac{\rho_R r_R}{r_0^2 \rho_c h} A_R X_{jv,R} X_{mv,R} + \Delta\beta_{jm,R} \tag{B17}$$

$$(\beta\gamma)_{jm,R} = \frac{\rho_R n}{r_0^2 \rho_c h} \left[\left(A_R z_R + \frac{I_{s,R}}{r_R} \cos\delta \right) X_{jv,R} X_{mw,R} - \left(I_{sz,R} + \frac{I_{1,R} \cos\delta}{r_R} \right) X_{jv,R} X'_{mw,R} \right] \tag{B18}$$

$$\gamma_{jm,R} = \frac{\rho_R r_R}{r_0^2 \rho_c h} A_R X_{jw,R} X_{mw,R} + \Delta\gamma_{jm,R} \tag{B19}$$

The subscript R with the symbols X and X' denotes evaluation of these modal functions at the ring location; for example, $X_{ju,R} = X_{ju}(s_R)$, $X'_{jw,R} = \frac{d}{ds} X_{jw}(s)\Big|_{s=s_R}$, and so forth. For consistency with the strain and kinetic energies in equations (6), (7), (14), and (15), the dominant or primary stiffness and mass-inertia parts of the elements are given first and are followed by the secondary parts, which are specified as follows:

$$\Delta A_{jm,R} = \left(\frac{n}{r_R} \right)^2 \left[2(EA)_R \hat{s}_R \sin\delta + (EI_z)_R \frac{n^2}{r_R} \right] X_{ju,R} X_{mu,R} \tag{B20}$$

$$\Delta B_{jm,R} = \frac{n^3}{r_R^2} \left[(EA)_R \hat{s}_R + (EI_{sz})_R \frac{\cos\delta}{r_R} \right] X_{ju,R} X_{mv,R} \tag{B21}$$

APPENDIX B

$$\Delta E_{jm,R} = \frac{1}{r_R}\Bigg[(EA)_R \hat{s}_R X_{ju,R} \cos\delta\left(\frac{n^2 X_{mw,R}}{r_R} + X'_{mw,R}\sin\delta\right) + (EI_{sz})_R \frac{n^2 X_{ju,R}}{r_R}\left(\frac{n^2 X_{mw,R}}{r_R} - 2X'_{mw,R}\sin\delta\right) + (EI_z)_R \frac{n^2 X_{ju,R} X'_{mw,R}\cos\delta}{r_R} - (EI_2)_R \frac{n^4 X_{ju,R} X'_{mw,R}}{r_R^2}\Bigg] \tag{B22}$$

$$\Delta G_{jm,R} = \frac{n}{r_R}\left[(EA)_R \hat{s}_R \cos\delta + \frac{(EI_{sz})_R}{r_R}(\cos^2\delta - n^2) - \frac{n^2 (EI_1)_R}{r_R^2}\cos\delta\right] X_{jv,R} X'_{mw,R} \tag{B23}$$

$$\Delta H_{jm,R} = \frac{1}{r_R}\Bigg\{(EA)_R \hat{s}_R \cos^2\delta\left(X'_{jw,R} X_{mw,R} + X_{jw,R} X'_{mw,R}\right) - (EI_{sz})_R X'_{jw,R} X'_{mw,R}\sin 2\delta - (EI_1)_R \frac{n^2}{r_R}\left[\frac{n^2}{r_R}\left(X'_{jw,R} X_{mw,R} + X_{jw,R} X'_{mw,R}\right) - 2X'_{jw,R} X'_{mw,R}\sin\delta\right] + (EI_z)_R X'_{jw,R} X'_{mw,R}\cos^2\delta - 2n^2 \frac{(EI_2)_R}{r_R} X'_{jw,R} X'_{mw,R}\cos\delta + n^4 (E\Gamma)_R \frac{X'_{jw,R} X'_{mw,R}}{r_R^2}\Bigg\} \tag{B24}$$

$$\Delta\alpha_{jm,R} = \frac{\rho_R n^2 I_{z,R}}{r_0^2 \rho h r_R} X_{ju,R} X_{mu,R} \tag{B25}$$

$$\Delta\beta_{jm,R} = \frac{\rho_R \cos\delta}{r_0^2 \rho h}\left(2A_R z_R + \frac{I_{s,R}}{r_R}\cos\delta\right) X_{jv,R} X_{mv,R} \tag{B26}$$

$$\Delta\gamma_{jm,R} = \frac{\rho_R r_R}{r_0^2 \rho h}\Bigg[\frac{n^2 I_{s,R}}{r_R^2} X_{jw,R} X_{mw,R} + \left(A_R \hat{s}_R - \frac{n^2 I_{1,R}}{r_R^2}\right)\left(X'_{jw,R} X_{mw,R} + X_{jw,R} X'_{mw,R}\right) + \left(J_{e,R} + \frac{\Gamma_R n^2}{r_R^2}\right) X'_{jw,R} X'_{mw,r}\Bigg] \tag{B27}$$

APPENDIX B

The off-diagonal elements of the mass-inertia matrix (eqs. (B15), (B16), and (B18)) are also considered secondary terms.

Mode-Shape Integrals

With $X_m = \left(\frac{s - s_1}{s_2 - s_1}\right)^m$, the number of integrals in equations (B1) to (B7) reduces to 14, each of which is evaluated as follows:

$$I_1 = \int_{s_1}^{s_2} X_j X_m s \, ds = L^2\left(\frac{1}{j + m + 2} + \frac{s_1}{L}\frac{1}{j + m + 1}\right)$$

$$I_2 = \int_{s_1}^{s_2} X_j X_m \frac{ds}{s} = \left(\frac{s_1}{L}\right)^{j+m}\left\{(j + m)!\sum_{k=0}^{j+m}\frac{(-1)^k\left[\left(\frac{s_2}{s_1}\right)^{j+m-k} - 1\right]}{(j + m - k)!\,k!\,(j + m - k)} + (-1)^{j+m}\log\frac{s_2}{s_1}\right\}$$

$$I_3 = \int_{s_1}^{s_2} X_j X_m \frac{ds}{s^3} = \frac{1}{L^2}\left(\frac{s_1}{L}\right)^{j+m-2}\left\{(j + m)!\sum_{k=0}^{j+m}\frac{(-1)^k\left[\left(\frac{s_2}{s_1}\right)^{j+m-2-k} - 1\right]}{(j + m - k)!\,k!\,(j + m - 2 - k)} + \frac{(-1)^{j+m-2}}{2}(j + m)(j + m - 1)\log\frac{s_2}{s_1}\right\}$$

$$I_4 = \int_{s_1}^{s_2} X_j' X_m \, ds = \frac{j}{j + m}$$

$$I_5 = \int_{s_1}^{s_2} X_j X_m' \, ds = \frac{m}{j + m}$$

$$I_6 = \int_{s_1}^{s_2} X_j' X_m' s \, ds = jm\left(\frac{1}{j + m} + \frac{s_1}{L}\frac{1}{j + m - 1}\right)$$

$$I_7 = \int_{s_1}^{s_2} X_j X_m' \frac{ds}{s^2} = \frac{m}{L^2}\left(\frac{s_1}{L}\right)^{j+m-2}\left\{(j + m - 1)!\sum_{k=0}^{j+m-1}\frac{(-1)^k\left[\left(\frac{s_2}{s_1}\right)^{j+m-2-k} - 1\right]}{(j + m - 1 - k)!\,k!\,(j + m - 2 - k)} + (-1)^{j+m-2}(j + m - 1)\log\frac{s_2}{s_1}\right\}$$

$$I_8 = \int_{s_1}^{s_2} X_j' X_m \frac{ds}{s^2} = \frac{j}{L^2}\left(\frac{s_1}{L}\right)^{j+m-2}\left\{(j + m - 1)!\sum_{k=0}^{j+m-1}\frac{(-1)^k\left[\left(\frac{s_2}{s_1}\right)^{j+m-2-k} - 1\right]}{(j + m - 1 - k)!\,k!\,(j + m - 2 - k)} + (-1)^{j+m-2}(j + m - 1)\log\frac{s_2}{s_1}\right\}$$

$$I_9 = \int_{s_1}^{s_2} X_j' X_m' \frac{ds}{s} = \frac{jm}{L^2}\left(\frac{s_1}{L}\right)^{j+m-2}\left\{(j + m - 2)!\sum_{k=0}^{j+m-2}\frac{(-1)^k\left[\left(\frac{s_2}{s_1}\right)^{j+m-2-k} - 1\right]}{(j + m - 2 - k)!\,k!\,(j + m - 2 - k)} + (-1)^{j+m-2}\log\frac{s_2}{s_1}\right\}$$

APPENDIX B

$$I_{10} = \int_{s_1}^{s_2} X_j X_m'' \frac{ds}{s} = \frac{m(m-1)}{L^2}\left(\frac{s_1}{L}\right)^{j+m-2} \left\{ (j+m-2)! \sum_{k=0}^{j+m-2} \frac{(-1)^k \left[\left(\frac{s_2}{s_1}\right)^{j+m-2-k} - 1\right]}{(j+m-2-k)!\, k!\, (j+m-2-k)} + (-1)^{j+m-2} \log \frac{s_2}{s_1} \right\}$$

$$I_{11} = \int_{s_1}^{s_2} X_j'' X_m \frac{ds}{s} = \frac{j(j-1)}{L^2}\left(\frac{s_1}{L}\right)^{j+m-2} \left\{ (j+m-2)! \sum_{k=0}^{j+m-2} \frac{(-1)^k \left[\left(\frac{s_2}{s_1}\right)^{j+m-2-k} - 1\right]}{(j+m-2-k)!\, k!\, (j+m-2-k)} + (-1)^{j+m-2} \log \frac{s_2}{s_1} \right\}$$

$$I_{12} = \int_{s_1}^{s_2} X_j' X_m'' \, ds = \frac{1}{L^2} \frac{jm(m-1)}{j+m-2}$$

$$I_{13} = \int_{s_1}^{s_2} X_j'' X_m' \, ds = \frac{1}{L^2} \frac{jm(j-1)}{j+m-2}$$

$$I_{14} = \int_{s_1}^{s_2} X_j'' X_m'' s \, ds = \frac{jm(j-1)(m-1)}{L^2}\left(\frac{1}{j+m-2} + \frac{s_1}{L}\frac{1}{j+m-3}\right)$$

Mode-Shape Functions of Ring

Power-series modal functions in equations (B8) to (B27) at the shell-ring interfaces involve the following functions:

$$X_{j,R} X_{m,R} = \left(\frac{s_R - s_1}{L}\right)^{j+m} \tag{B28}$$

$$X_{j,R} X'_{m,R} = \frac{m}{L}\left(\frac{s_R - s_1}{L}\right)^{j+m-1} \tag{B29}$$

$$X'_{j,R} X_{m,R} = \frac{j}{L}\left(\frac{s_R - s_1}{L}\right)^{j+m-1} \tag{B30}$$

$$X'_{j,R} X'_{m,R} = \frac{jm}{L^2}\left(\frac{s_R - s_1}{L}\right)^{j+m-2} \tag{B31}$$

APPENDIX C

MATRIX ELEMENTS OF APPROXIMATE RING FREQUENCY EQUATION

This appendix contains pertinent details of the derivation of the approximate frequency equation of the conically oriented free ring as given by equation (20). Included are the basic strain-displacement relationships, strain and kinetic energies, and elements of the stiffness and mass-inertia matrices.

Strain-Displacement Relations

The strain-displacement relations for the free ring are developed in the same manner as those for the ring attached to the shell (appendix A) except that $\left(-\frac{\partial w}{\partial s}\right)_R$ is replaced by β_R, and $\left(\frac{\partial v}{\partial s}\right)_R$ is omitted from the torsional curvature term $\bar{\kappa}_{12}$. Thus, the basic strain-displacement relationships for an approximate ring frequency equation may be written as

$$e_{22,R} = \frac{1}{r_R}\left(\frac{\partial v}{\partial \phi} + u \sin \delta + w \cos \delta\right)_R + \frac{z}{r_R}\left[\frac{1}{r_R}\left(\frac{\partial v_R}{\partial \phi} \cos \delta - \frac{\partial^2 w_R}{\partial \phi^2}\right) + \beta_R \sin \delta\right]$$

$$- \frac{\hat{s}}{r_R}\left(\frac{\partial^2 u_R}{r_R\, \partial \phi^2} + \beta_R \cos \delta + z \frac{\partial^2 \beta_R}{r_R\, \partial \phi^2}\right) \tag{C1}$$

$$\bar{\kappa}_{12,R} = \frac{\partial \beta_R}{r_R\, \partial \phi} - \frac{3 v_R \cos \delta \sin \delta}{4 r_R^2} + \frac{\sin \delta}{r_R^2} \frac{\partial w_R}{\partial \phi} - \frac{\cos \delta}{4 r_R^2} \frac{\partial u_R}{\partial \phi} \tag{C2}$$

Strain Energy

The strain energy of the conically oriented free ring is developed by substituting equations (C1) and (C2) into the expression

$$U_R = \frac{1}{2} \int_0^{2\pi} \int_{A_R} E_R e_{22,R}^2 \, dA_R \, r_R \, d\phi + \frac{(GJ)_R}{2} \int_0^{2\pi} \bar{\kappa}_{12,R}^2 \, r_R \, d\phi \tag{C3}$$

to give

$$U_R = \frac{1}{2r_R}\int_0^{2\pi}\Bigg[(EA)_R\left(\frac{\partial v}{\partial\phi} + u\sin\delta + w\cos\delta\right)_R^2 + 2(EA)_R z_R\left(\frac{\partial v}{\partial\phi} + u\sin\delta + w\cos\delta\right)_R\left(\frac{\partial v_R}{r_R\,\partial\phi}\cos\delta - \frac{1}{r_R}\frac{\partial^2 w_R}{\partial\phi^2} + \beta_R\sin\delta\right)$$

$$+ (EI_s)_R\left(\frac{\partial v}{r_R\,\partial\phi}\cos\delta - \frac{1}{r_R}\frac{\partial^2 w_R}{\partial\phi^2} + \beta_R\sin\delta\right)^2\Bigg]d\phi + \frac{(GJ)_R}{2r_R}\int_0^{2\pi}\left(\frac{\partial\beta_R}{\partial\phi} - \frac{3v_R\cos\delta\sin\delta}{4r_R} + \frac{\sin\delta}{r_R}\frac{\partial w_R}{\partial\phi} - \frac{\cos\delta}{4r_R}\frac{\partial u_R}{\partial\phi}\right)^2 d\phi$$

$$+ \frac{1}{2}\int_0^{2\pi}\Bigg\{-2(EA)_R\frac{\hat{s}_R}{r_R}\left(\frac{\partial v}{\partial\phi} + u\sin\delta + w\cos\delta\right)_R\left(\frac{\partial^2 u_R}{r_R\,\partial\phi^2} + \beta_R\cos\delta\right) - 2\frac{(EI_{sz})_R}{r_R}\Bigg[\left(\frac{\partial v_R}{r_R\,\partial\phi}\cos\delta - \frac{\partial^2 w_R}{r_R\,\partial\phi^2}\right.$$

$$\left.+ \beta_R\sin\delta\right)\left(\frac{\partial^2 u_R}{r_R\,\partial\phi^2} + \beta_R\cos\delta\right) + \left(\frac{\partial v}{\partial\phi} + u\sin\delta + w\cos\delta\right)_R\frac{\partial^2\beta_R}{r_R\,\partial\phi^2}\Bigg] - 2\frac{(EI_1)_R}{r_R^2}\left(\frac{\partial v_R}{r_R\,\partial\phi}\cos\delta - \frac{1}{r_R}\frac{\partial^2 w_R}{\partial\phi^2} + \beta_R\sin\delta\right)\frac{\partial^2\beta_R}{\partial\phi^2}$$

$$+ 2\frac{(EI_2)_R}{r_R^2}\left(\frac{\partial^2 u_R}{r_R\,\partial\phi^2} + \beta_R\cos\delta\right)\frac{\partial^2\beta_R}{\partial\phi^2} + \frac{(EI_z)_R}{r_R}\left(\frac{\partial^2 u_R}{r_R\,\partial\phi^2} + \beta_R\cos\delta\right)^2 + \frac{(E\Gamma)_R}{r_R^3}\left(\frac{\partial^2\beta_R}{\partial\phi^2}\right)^2\Bigg\}d\phi \qquad \text{(C4)}$$

where the cross-sectional properties $A_R, \ldots, \Gamma_R$ are defined in equations (8).

Kinetic Energy

The free-ring kinetic energy is given by

$$T_R = \frac{\rho_R}{2}\int_0^{2\pi}\int_{A_R}\left(\dot{\bar{u}}_t^2 + \dot{\bar{v}}_t^2 + \dot{\bar{w}}_t^2\right)dA_R\, r_R\, d\phi \qquad \text{(C5)}$$

where

$$\left.\begin{aligned}\dot{\bar{u}}_t &= \dot{u}_R + z\dot{\beta}_R\\ \dot{\bar{v}}_t &= \dot{v}_R + \frac{z}{r_R}\left(\dot{v}_R\cos\delta - \frac{\partial\dot{w}_R}{\partial\phi}\right) - \frac{\hat{s}}{r_R}\left(\frac{\partial\dot{u}_R}{\partial\phi} + z\frac{\partial\dot{\beta}_R}{\partial\phi}\right)\\ \dot{\bar{w}}_t &= \dot{w}_R - \hat{s}\dot{\beta}_R\end{aligned}\right\} \qquad \text{(C6)}$$

Substitution of equations (C6) into equation (C5) leads to

$$T_R = \frac{\rho_R}{2}\int_0^{2\pi}\Bigg\{A_R\left(\dot{u}_R^2 + \dot{v}_R^2 + \dot{w}_R^2\right) + 2A_R z_R\left[\dot{u}_R\dot{\beta}_R + \frac{\dot{v}_R}{r_R}\left(\dot{v}_R\cos\delta - \frac{\partial\dot{w}_R}{\partial\phi}\right)\right]$$

$$- 2A_R\hat{s}_R\left(\frac{\dot{v}_R}{r_R}\frac{\partial\dot{u}_R}{\partial\phi} + \dot{w}_R\dot{\beta}_R\right) + J_{e,R}\dot{\beta}_R^2 + \frac{I_{s,R}}{r_R^2}\left(\dot{v}_R\cos\delta - \frac{\partial\dot{w}_R}{\partial\phi}\right)^2$$

$$+ \frac{I_{z,R}}{r_R^2}\left(\frac{\partial\dot{u}_R}{\partial\phi}\right)^2 - 2\frac{I_{sz,R}}{r_R}\left[\dot{v}_R\frac{\partial\dot{\beta}_R}{\partial\phi} + \frac{1}{r_R}\frac{\partial\dot{u}_R}{\partial\phi}\left(\dot{v}_R\cos\delta - \frac{\partial\dot{w}_R}{\partial\phi}\right)\right]$$

$$- 2\frac{I_{1,R}}{r_R^2}\frac{\partial\dot{\beta}_R}{\partial\phi}\left(\dot{v}_R\cos\delta - \frac{\partial\dot{w}_R}{\partial\phi}\right) + 2\frac{I_{2,R}}{r_R^2}\frac{\partial\dot{u}_R}{\partial\phi}\frac{\partial\dot{\beta}_R}{\partial\phi} + \frac{\Gamma_R}{r_R^2}\left(\frac{\partial\dot{\beta}_R}{\partial\phi}\right)^2\Bigg\}r_R\,d\phi \qquad \text{(C7)}$$

Matrix Elements

With the substitution of equations (19) into equations (C4) and (C7), the equations of motion are obtained from the following relations, which are essentially the ring portions of equations (17):

$$\left.\begin{aligned}
&\frac{\partial}{\partial\bar{a}_{n,R}}\left(U_R - \omega^2 T_R\right) = 0\\
&\frac{\partial}{\partial\bar{b}_{n,R}}\left(U_R - \omega^2 T_R\right) = 0\\
&\frac{\partial}{\partial\bar{c}_{n,R}}\left(U_R - \omega^2 T_R\right) = 0\\
&\frac{\partial}{\partial\bar{d}_{n,R}}\left(U_R - \omega^2 T_R\right) = 0
\end{aligned}\right\} \qquad \text{(C8)}$$

The operations indicated in equations (C8) lead to equation (20), where the elements of the stiffness and mass matrices are as follows:

$$K_{11} = (EA)_R\sin^2\delta + n^2\frac{(GJ)_R\cos^2\delta}{16r_R^2} + n^2\left[2(EA)_R\frac{\hat{s}_R}{r_R}\sin\delta + n^2\frac{(EI_z)_R}{r_R^2}\right] \qquad \text{(C9)}$$

APPENDIX C

$$K_{12} = K_{21} = n \sin\delta\left[(EA)_R\left(1 + \frac{z_R}{r_R}\cos\delta\right) - 3\frac{(GJ)_R\cos^2\delta}{16r_R^2}\right] + n^3\left[(EA)_R\frac{\hat{s}_R}{r_R} + \frac{(EI_{sz})_R}{r_R^2}\cos\delta\right] \quad \text{(C10)}$$

$$K_{13} = K_{31} = (EA)_R \sin\delta\cos\delta + n^2\frac{(EA)_R}{r_R}\left(z_R\sin\delta + \hat{s}_R\cos\delta\right) - n^2\frac{(GJ)_R\sin\delta\cos\delta}{4r_R^2} + n^4\frac{(EI_{sz})_R}{r_R^2} \quad \text{(C11)}$$

$$K_{14} = K_{41} = (EA)_R\sin\delta\left(z_R\sin\delta - \hat{s}_R\cos\delta\right) - n^2\frac{(GJ)_R\cos\delta}{4r_R}$$

$$+ \frac{n^2}{r_R}\left[2(EI_{sz})_R\sin\delta - (EI_z)_R\cos\delta + n^2\frac{(EI_2)_R}{r_R}\right] \quad \text{(C12)}$$

$$K_{22} = n^2\left[(EA)_R\left(1 + 2\frac{z_R}{r_R}\cos\delta\right) + \frac{(EI_s)_R}{r_R^2}\cos^2\delta\right] + \frac{9(GJ)_R\sin^2\delta\cos^2\delta}{16r_R^2} \quad \text{(C13)}$$

$$K_{23} = K_{32} = n\left\{(EA)_R\left[\cos\delta + \frac{z_R}{r_R}\left(n^2 + \cos^2\delta\right)\right] + n^2\frac{(EI_s)_R\cos\delta}{r_R^2} + \frac{3(GJ)_R\sin^2\delta\cos\delta}{4r_R^2}\right\} \quad \text{(C14)}$$

$$K_{24} = K_{42} = n(EA)_R\left(z_R\sin\delta - \hat{s}_R\cos\delta\right) + n\frac{\sin\delta\cos\delta}{r_R}\left[(EI_s)_R + \frac{3(GJ)_R}{4}\right]$$

$$+ \frac{n}{r_R}\left[(EI_{sz})_R\left(n^2 - \cos^2\delta\right) + n^2\frac{(EI_1)_R\cos\delta}{r_R}\right] \quad \text{(C15)}$$

$$K_{33} = (EA)_R\cos\delta\left(\cos\delta + 2n^2\frac{z_R}{r_R}\right) + n^4\frac{(EI_s)_R}{r_R^2} + n^2\frac{(GJ)_R\sin^2\delta}{r_R^2} \quad \text{(C16)}$$

$$K_{34} = K_{43} = (EA)_R\cos\delta\left(z_R\sin\delta - \hat{s}_R\cos\delta\right) + n^2\frac{\sin\delta}{r_R}\left[(EI_s)_R + (GJ)_R\right] + n^4\frac{(EI_1)_R}{r_R^2} \quad \text{(C17)}$$

$$K_{44} = (EI_s)_R\sin^2\delta + (EI_z)_R\cos^2\delta - (EI_{sz})_R\sin 2\delta$$

$$+ 2\frac{n^2}{r_R}\left[(EI_1)_R\sin\delta - (EI_2)_R\cos\delta\right] + n^2\left[(GJ)_R + n^2\frac{(EI')_R}{r_R^2}\right] \quad \text{(C18)}$$

$$M_{11} = 1 + n^2 \frac{I_{z,R}}{A_R r_R^2} \tag{C19}$$

$$M_{12} = M_{21} = n\left(\frac{\hat{s}_R}{r_R} + \frac{I_{sz,R} \cos \delta}{A_R r_R^2}\right) \tag{C20}$$

$$M_{13} = M_{31} = n^2 \frac{I_{sz,R}}{A_R r_R^2} \tag{C21}$$

$$M_{14} = M_{41} = z_R + n^2 \frac{I_{2,R}}{A_R r_R^2} \tag{C22}$$

$$M_{22} = 1 + 2 \frac{z_R}{r_R} \cos \delta + \frac{I_{s,R} \cos^2 \delta}{A_R r_R^2} \tag{C23}$$

$$M_{23} = M_{32} = n\left(\frac{z_R}{r_R} + \frac{I_{s,R} \cos \delta}{A_R r_R^2}\right) \tag{C24}$$

$$M_{24} = M_{42} = n\left(\frac{I_{sz,R}}{A_R r_R} + \frac{I_{1,R} \cos \delta}{A_R r_R^2}\right) \tag{C25}$$

$$M_{33} = 1 + n^2 \frac{I_{s,R}}{A_R r_R^2} \tag{C26}$$

$$M_{34} = M_{43} = -\hat{s}_R + n^2 \frac{I_{1,R}}{A_R r_R^2} \tag{C27}$$

$$M_{44} = \frac{J_{e,R}}{A_R} + n^2 \frac{\Gamma_R}{A_R r_R^2} \tag{C28}$$

In equations (C19) to (C28), the primary mass-inertia effects are given by $M_{11} = M_{22} = M_{33} = 1$ and $M_{44} = J_{e,R}/A_R$. All other terms in these equations are considered secondary inertias, which are shown in table V to have a negligible effect on the frequencies of the free Z-rings.

REFERENCES

1. McGrattan, R. J.; and North, E. L.: Shell Mode Coupling – Final Report (1962). U411-63-005 (NOnr 3594(00)), Gen. Dyn./Elec. Boat, Mar. 1963.

2. Hung, F. C.; Park, A. C.; Chan, C.; Andrew, L. V.; and Au, L. L. T.: Dynamics of Shell-Like Lifting Bodies. AFFDL-TR-65-17, Pts. I and II, U.S. Air Force, June 1965.
   Part I. The Analytical Investigation. (Available from DDC as AD 621 146.)
   Part II. The Experimental Investigation. (Available from DDC as AD 620 699.)

3. Weingarten, V. I.: Free Vibrations of Ring-Stiffened Conical Shells. AIAA J., vol. 3, no. 8, Aug. 1965, pp. 1475-1481.

4. McMunn, John C.: Vibration Analysis of the Ring-Stiffened Conical Shell Gemini Adapter. SDPN 236-52-7A, McDonnell Aircraft Corp., Aug. 1963. (Rev. Feb. 1965 by J. W. Dick.)

5. Crenwelge, Otto E., Jr.; and Muster, D.: Free Vibrations of Ring-and-Stringer-Stiffened Conical Shells. Tech. Rep. No. 9 (Contract Nonr-4492(0)), Dep. Mech. Eng., Univ. of Houston, Apr. 1968. (Available from DDC as AD 669 499.)

6. Newton, Roland A.: Free Vibrations of Rocket Nozzles. AIAA Symposium on Structural Dynamics and Aeroelasticity, Aug.-Sept. 1965, pp. 400-405.

7. Naumann, Eugene C.: On the Prediction of the Vibratory Behavior of Free-Free Truncated Conical Shells. NASA TN D-4772, 1968.

8. Mikulas, Martin M., Jr.; and McElman, John A.: On Free Vibrations of Eccentrically Stiffened Cylindrical Shells and Flat Plates. NASA TN D-3010, 1965.

9. McElman, John A.: Eccentrically Stiffened Shallow Shells. Ph. D. Thesis, Virginia Polytech. Inst., 1966.

10. Sanders, J. Lyell, Jr.: An Improved First-Approximation Theory for Thin Shells. NASA TR R-24, 1959.

11. White, Paul A.: The Computation of Eigenvalues and Eigenvectors of a Matrix. J. Soc. Ind. Appl. Math., vol. 6, no. 4, Dec. 1958, pp. 393-437.

TABLE I.- GEOMETRICAL AND STRUCTURAL PROPERTIES OF SHELL AND RINGS

(a) Conical shell

r_1, including base ring	3 in. (76.2 mm)
r_2	24 in. (60.96 cm)
E_c	10^7 lb/in^2 (68.95 GN/m^2)
h	0.025 in. (0.635 mm)
δ	60^o
μ	0.315
ρ_c	2.54×10^{-4} lb-sec^2/in^4 (7.02 kg/m^3)

(b) Rings

E_R	10^7 lb/in^2 (68.95 GN/m^2)
G_R	3.8×10^6 lb/in^2 (26.2 GN/m^2)
ρ_R	2.54×10^{-4} lb-sec^2/in^4 (7.02 kg/m^3)

Property (eqs. (8))	Base ring	Z-ring	
		Attached to shell	Free
s_R	4.0425 in. (102.7 mm)	27.51 in. (69.9 cm)	27.33 in. (69.4 cm)
		15.98 in. (40.6 cm)	15.80 in. (40.13 cm)
$\hat{s}_R$	0	0.164 in. (4.166 mm)	0
z_R	-0.0625 in. (-1.587 mm)	-0.6025 in. (-15.3 mm)	0
A_R	0.1155 in^2 (74.5 mm^2)	0.0955 in^2 (61.6 mm^2)	0.0955 in^2 (61.6 mm^2)
$I_{s,R}$	0.5473×10^{-3} in^4 (0.02278 cm^4)	0.05273 in^4 (2.195 cm^4)	0.0180 in^4 (0.749 cm^4)
$I_{sz,R}$	0	-0.01305 in^4 (-0.543 cm^4)	-0.003655 in^4 (-0.152 cm^4)
$I_{z,R}$	0.01284 in^4 (0.534 cm^4)	0.00411 in^4 (0.171 cm^4)	0.001551 in^4 (0.0646 cm^4)
$I_{1,R}$	0	0.01332 in^5 (1.408 cm^5)	0
$I_{2,R}$	-0.802×10^{-3} in^5 (-0.0848 cm^5)	-0.00367 in^5 (-0.3880 cm^5)	0
J_R	0.366×10^{-3} in^4 (0.01523 cm^4)	0.86×10^{-4} in^4 (0.003580 cm^4)	0.86×10^{-4} in^4 (0.003580 cm^4)
$J_{e,R}$	0.013387 in^4 (0.5572 cm^4)	0.05684 in^4 (2.366 cm^4)	0.019551 in^4 (0.814 cm^4)
Γ_R	0.6085×10^{-4} in^6 (0.01634 cm^6)	0.004027 in^6 (1.08 cm^6)	4.910×10^{-4} in^6 (0.13185 cm^6)

TABLE II.- ANALYTICAL AND EXPERIMENTAL FREQUENCIES OF SHELL WITH BASE RING

n	Analytical frequency, Hz										[a]Experimental frequency, Hz
	Without ring secondary stiffnesses and inertias								Wing ring secondary stiffnesses and inertias		
	6 w-terms 7 u- and v-terms		9 w-terms 10 u- and v-terms		12 w-terms 13 u- and v-terms		14 w-terms 15 u- and v-terms		12 w-terms 13 u- and v-terms		
	m = 1	m = 2	m = 1	m = 2	m = 1	m = 2	m = 1	m = 2	m = 1	m = 2	m = 1
0	[b]253.6	706.3	[b]253.5	697.0	[b]253.5	696.3	[b]253.5	696.2	[b]253.5	696.4	
	516.2		513.8		513.7		513.6		515.2		
1	102.4	696.7	97.3	689.8	96.4	689.4	96.3	689.3	100.6	689.4	
2	46.2	562.8	43.6	554.5	43.1	552.1	43.1	551.4	46.2	562.7	43.8
3	25.6	357.5	25.0	349.6	25.0	348.7	25.0	348.3	25.9	359.8	25.4
4	19.6	241.1	19.5	238.5	19.4	237.9	19.4	237.9	19.5	241.6	19.6
5	21.5	181.1	21.4	179.3	21.4	177.5	21.4	177.2	21.4	178.2	21.0
6	27.0	153.3	26.9	150.3	26.9	148.9	26.9	148.9	26.9	149.1	26.7
7	33.7	143.0	33.6	140.9	33.6	140.6	33.6	140.6	33.6	140.7	33.1
											33.7
8	41.2	142.4	41.0	142.1	41.0	142.1	41.0	142.1	41.0	142.1	40.6
											41.3
9	49.3	147.6	49.2	147.4	49.2	147.4	49.2	147.4	49.2	147.4	47.9
											49.3
10	58.3	155.3	58.1	155.0	58.1	155.0	58.1	155.0	58.1	155.0	57.8
											58.5
11	68.0	164.5	67.9	164.4	67.9	164.3	67.9	164.3	67.9	164.3	67.0
											68.6
12	78.7	175.6	78.5	175.3	78.4	175.3	78.4	175.3	78.4	175.3	78.6
											79.2
13	90.2	188.7	89.9	187.8	89.9	187.8	89.9	187.8	89.9	187.8	89.3
											90.6
14	102.6	203.5	102.2	201.7	102.2	201.7	102.2	201.7	102.2	201.7	101.4
											102
15	116.0	219.2	115.4	216.9	115.3	216.9	115.3	216.9	115.3	216.9	113.5
											115

[a]From an unpublished study by Eugene C. Naumann, John S. Mixson, and Earl C. Steeves.

[b]Torsion (or v) mode.

TABLE III.- ANALYTICAL AND EXPERIMENTAL FREQUENCIES OF CONICAL SHELL WITH BASE RING AND ONE Z-RING AT THE FREE END

n	Analytical frequency, Hz												[a]Experimental frequency, Hz	
	Without ring secondary stiffnesses and inertias								With ring secondary stiffnesses and inertias		With ring secondary stiffnesses			
	9 w-terms 10 u- and v-terms		12 w- terms 13 u- and v-terms		16 w-terms 17 u- and v-terms		17 w-terms 18 u- and v-terms		16 w-terms 17 u- and v-terms		16 w-terms 17 u- and v-terms			
	m = 1	m = 2	m = 1	m = 2	m = 1	m = 2	m = 1	m = 2	m = 1	m = 2	m = 1	m = 2	m = 1	m = 2
0	[b]203.6	643.6	[b]203.6	636.7	[b]203.6	630.6	[b]203.6	630.2	[b]204.5	637.2	[b]203.6	625.8		
	419.4		417.8		414.8		414.6		408.3		412.5			
1	78.0	600.0	77.2	592.9	77.2	584.8	77.1	584.3	79.8	567.5	80.1	577.2		
2	37.7	481.4	37.0	478.2	36.7	475.2	36.6	475.1	37.9	478.5	38.4	479.6	38.2	
3	50.1	308.3	48.4	307.7	45.8	306.1	45.8	305.5	41.0	313.7	42.4	314.9	42.5	309.1
4	95.5	213.3	92.2	212.6	86.8	212.2	86.6	211.5	71.0	210.2	75.8	214.1	80.5	208.9
														211.2
5	131.8	204.2	129.6	198.6	125.6	193.2	125.6	192.3	108.2	163.7	115.3	177.8	123	178.4
														179.0
6	120.3	290.0	119.2	281.8	118.2	271.4	118.2	270.0	116.2	189.6	116.8	231.5	116.6	242.1
7	116.0	293.2	115.7	291.2	115.3	288.8	115.3	287.9	114.9	248.9	114.9	279.9	115.3	276.5
8	119.0	276.1	118.9	275.7	118.6	274.6	118.6	274.3	118.6	271.5	118.6	273.0	116.9	264.8
9	125.2	269.4	125.1	269.2	124.8	268.4	124.8	268.3	125.0	267.9	125.0	267.9	123.2	
10	133.4	268.7	133.3	268.5	133.0	267.8	132.9	267.8	133.3	267.8	133.3	267.8	130.7	258.1
														261.3
11	143.3	272.2	143.1	272.0	142.7	271.3	142.7	271.2	143.2	271.5	143.2	271.5	139.6	265.9
12	154.7	279.0	154.5	278.7	154.0	278.0	154.0	278.0	154.6	278.4	154.6	278.4	150.4	
13	167.4	288.6	167.2	288.3	166.7	287.6	166.6	287.5	167.3	288.0	167.3	288.0	162.3	
14	181.5	300.8	181.3	300.3	180.6	299.5	180.6	299.4	181.4	300.1	181.4	300.1	175.5	290.2
														295.9
15	196.9	315.0	196.6	314.5	195.9	313.6	195.8	313.5	196.7	314.3	196.7	314.3	187.2	
16	213.5	331.1	213.1	330.7	212.3	329.7	212.3	329.6	213.3	330.5	213.3	330.5	201.9	
17	231.3	349.2	230.9	348.8	230.0	347.7	229.9	347.6	231.0	348.5	231.0	348.5	221.4	
18	250.3	369.6	249.8	368.7	248.8	367.4	248.7	367.2	249.9	368.3	249.9	368.3	243.0	

[a]From an unpublished study by Eugene C. Naumann, John S. Mixson, and Earl C. Steeves.

[b]Torsion (or v) mode.

TABLE IV.- ANALYTICAL AND EXPERIMENTAL FREQUENCIES OF CONICAL SHELL WITH BASE RING AND TWO Z-RINGS

n	Analytical frequency, Hz												[a]Experimental frequency, Hz	
	Without ring secondary stiffnesses and inertias								With ring secondary stiffnesses and inertias		With ring secondary stiffnesses			
	13 w-terms 14 u- and v-terms		15 w-terms 16 u- and v-terms		17 w-terms 18 u- and v-terms		18 w-terms 19 u- and v-terms		17 w-terms 18 u- and v-terms		17 w-terms 18 u- and v-terms			
	m = 1	m = 2	m = 1	m = 2	m = 1	m = 2	m = 1	m = 2	m = 1	m = 2	m = 1	m = 2	m = 1	m = 2
0	[b]197.1	619.6	[b]197.1	618.9	[b]197.1	615.7	[b]197.1	615.6	[b]198.2	620.7	[b]197.1	610.4		
	412.5		409.4		409.3		409.0		402.6		406.7			
1	74.9	574.9	74.8	572.3	74.8	569.6	74.8	569.3	76.9	553.9	77.3	562.6	70.4	
2	61.4	446.1	57.2	438.8	54.9	438.5	53.7	436.7	50.0	437.1	50.8	441.6	40.3	
3	96.5	415.3	91.5	393.0	90.0	380.0	89.3	372.6	77.4	346.7	80.5	357.8	60.1	286.0
4	118.5	454.2	114.5	437.8	114.4	424.6	114.3	420.2	94.7	367.7	102.8	382.7	102.0	399
5	181.3	418.5	175.9	412.0	174.9	403.3	174.7	402.0	129.6	373.6	149.4	384.1	159.0	330.0
6	270.8	361.0	263.6	359.6	261.8	354.2	261.7	353.3	183.0	344.3	222.2	354.9	235.6	307.0
7	281.7	339.7	278.9	338.1	278.1	332.8	278.1	332.4	242.1	312.1	270.7	334.1	263.5	307.0
8	253.0	337.2	251.5	336.1	250.6	332.9	250.6	332.7	254.6	336.8	256.6	336.8	245.8	316.0
														326.0
9	228.2	351.1	227.2	349.8	226.2	348.0	226.1	347.9	235.1	354.7	235.3	354.8	211.5	342
													216.0	
10	210.2	374.8	209.5	373.1	208.4	371.8	208.2	371.7	217.9	381.3	218.0	381.4	200	359.0
11	199.0	404.7	198.4	402.4	197.2	401.2	197.1	401.2	206.0	413.3	206.1	413.4	183.2	399.0
12	193.9	418.1	193.4	413.4	192.2	412.7	192.0	411.4	199.7	426.7	199.7	426.8		438.0
13	194.1	405.4	193.7	400.2	192.5	399.2	192.3	397.7	198.5	412.6	198.5	412.6	178.0	
14	199.0	396.4	198.7	390.8	197.5	389.8	197.4	388.0	202.2	402.1	202.2	402.2		
15	207.8	392.0	207.6	386.1	206.5	385.2	206.4	383.53	210.1	396.3	210.1	396.4	201	
16	219.9	392.2	219.8	386.2	218.8	385.4	218.7	383.54	221.5	395.2	221.5	395.2	211	
													217	
17	234.8	396.7	234.6	390.8	233.7	390.1	233.7	389.3	235.9	398.6	235.8	398.6	226	
18	251.8	405.2	251.7	399.6	250.9	399.1	250.8	396.3	252.6	406.4	252.6	406.4	246	
19	270.8	417.5	270.6	412.3	269.8	412.0	269.8	410.8	271.3	418.1	271.3	418.1	264	400
20	291.4	433.2	291.1	428.5	290.4	428.4	290.4	427.8	291.7	433.5	291.7	433.5	286	
21	313.4	451.9	312.9	448.0	312.3	447.9	312.2	447.6	313.6	452.1	313.6	452.1	309	
													315	
22	336.6	473.5	336.0	470.2	335.4	470.1	335.3	468.8	336.7	473.6	336.7	473.6	327	
													330	
													343	

[a]From an unpublished study by Eugene C. Naumann, John S. Mixson, and Earl C. Steeves.

[b]Torsion (or v) mode.

TABLE V.- ANALYTICAL AND EXPERIMENTAL FREQUENCIES

OF CONICALLY ORIENTED FREE Z-RINGS

n	Analytical frequency, Hz						[a]Experimental frequency, Hz	
	With ring secondary stiffnesses and inertias				With ring secondary stiffnesses			
	1st mode	Dominant eigenvector	2d mode	Dominant eigenvector	1st mode	2d mode	1st mode	2d mode
				(a) Large Z-ring				
0	0	w_R	0.34	v_R	0	0.34		
1	.24	w_R	2.83	v_R	.24	2.83		
2	6.97	w_R	17.9	u_R	6.98	17.9	8.8	16.2
3	27.0	w_R	44.9	u_R	27.1	44.9	25.0	46.4
4	64.8	u_R	86.2	w_R	64.9	86.3	64.2	90.3
5	115.7	u_R	151.1	w_R	115.9	151.5	107.1	153.6
6	174.2	u_R	245.6	β_R	174.4	246.4	161.2	244.6
7	241.5	u_R	364.9	β_R	241.7	366.3	223.1	357
8	318.4	u_R	503.0	β_R	318.7	505.2	295.7	
9	405.2	u_R	655.9	β_R	405.6	658.7		
10	502.0	u_R	821.3	β_R	502.5	824.7		
				(b) Small Z-ring				
0	0	w_R	1.01	v_R	0	1.01		
1	.95	w_R	8.47	v_R	.95	8.47		
2	22.8	w_R	53.6	u_R	22.9	53.6	21.2	41.4
3	90.2	w_R	135.0	u_R	90.5	135.1	86.5	126
4	210.9	u_R	266.2	w_R	211.8	266.8	190	251
5	358.4	u_R	477.6	β_R	359.2	480.2	315	443
6	529.5	u_R	759.2	β_R	530.4	764.4	472	
7	728.9	u_R	1091	β_R	730.1	1099	668	

[a]From an unpublished study by Eugene C. Naumann, John S. Mixson, and Earl C. Steeves.

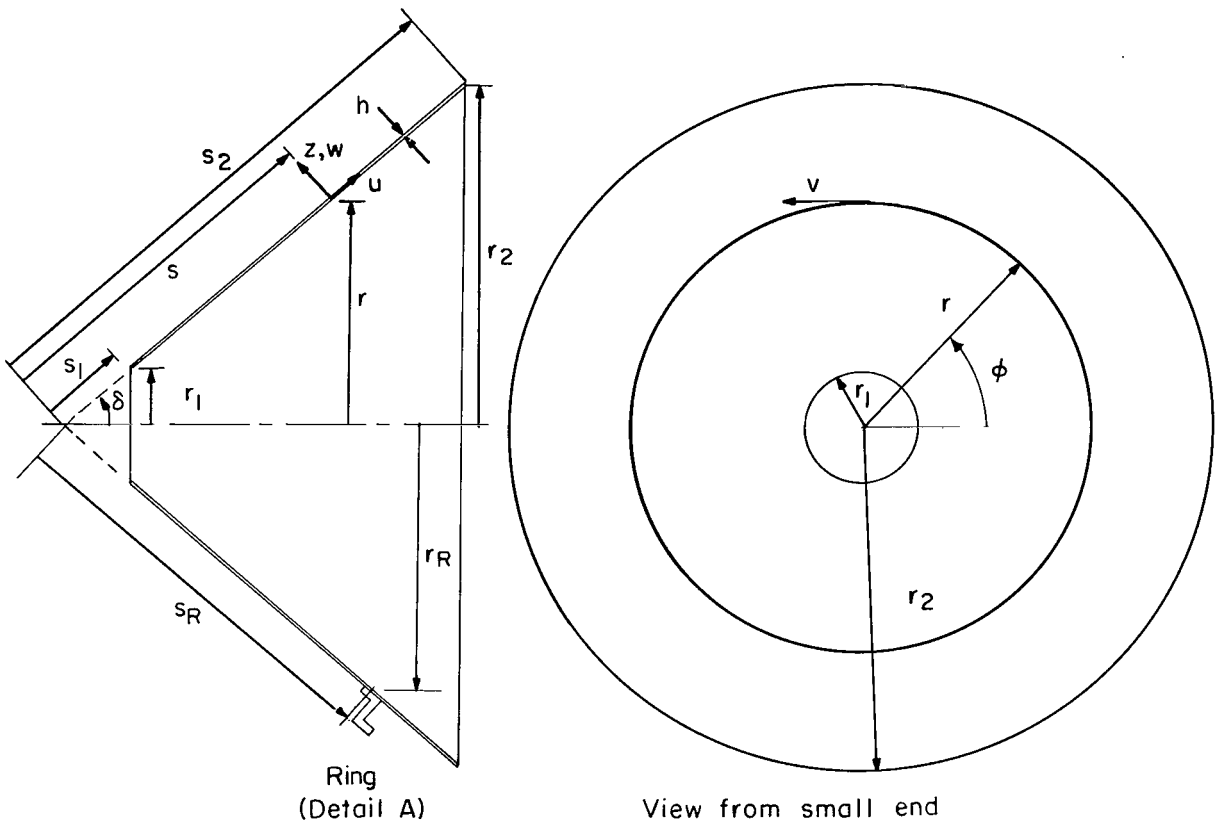

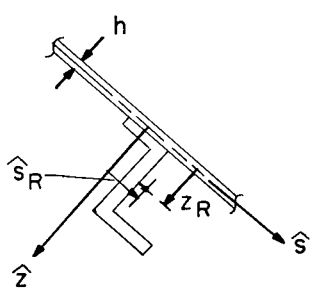

Detail A

(a) Ring-stiffened conical shell.

Figure 1.- Geometry and coordinates of conical shell and ring.

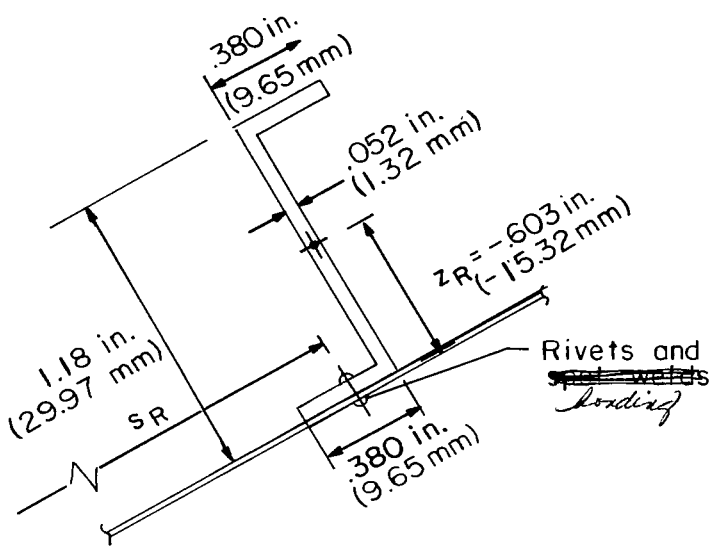

Z-ring

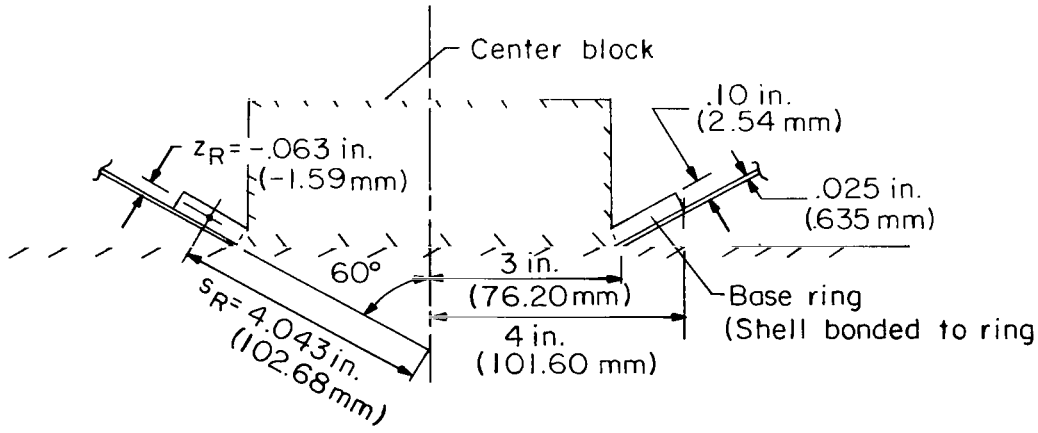

Base ring

(b) Geometrical details of ring stiffeners.

Figure 1.- Concluded.

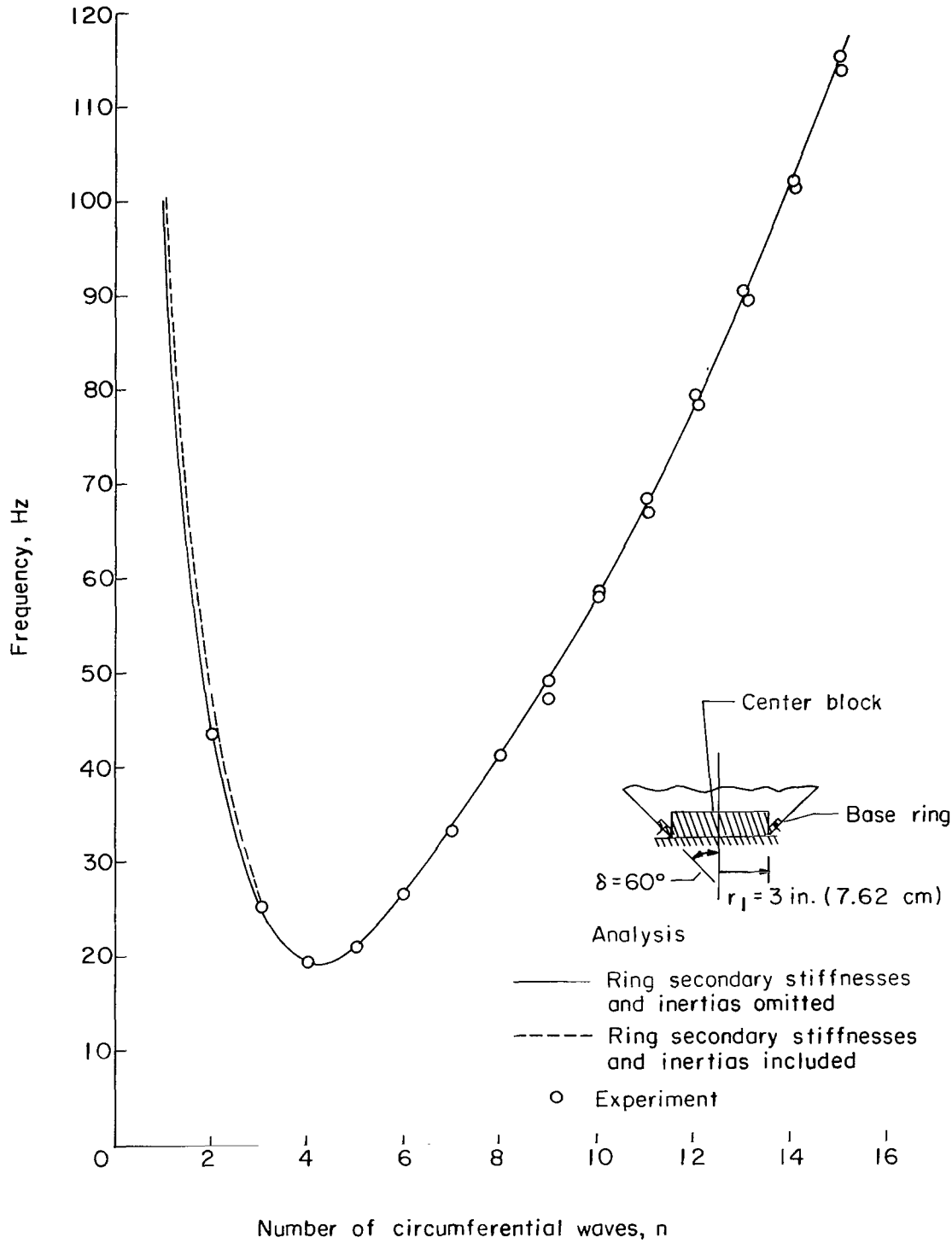

Figure 2.- Frequencies of 60^0 clamped-free conical shell with base ring for m = 1.

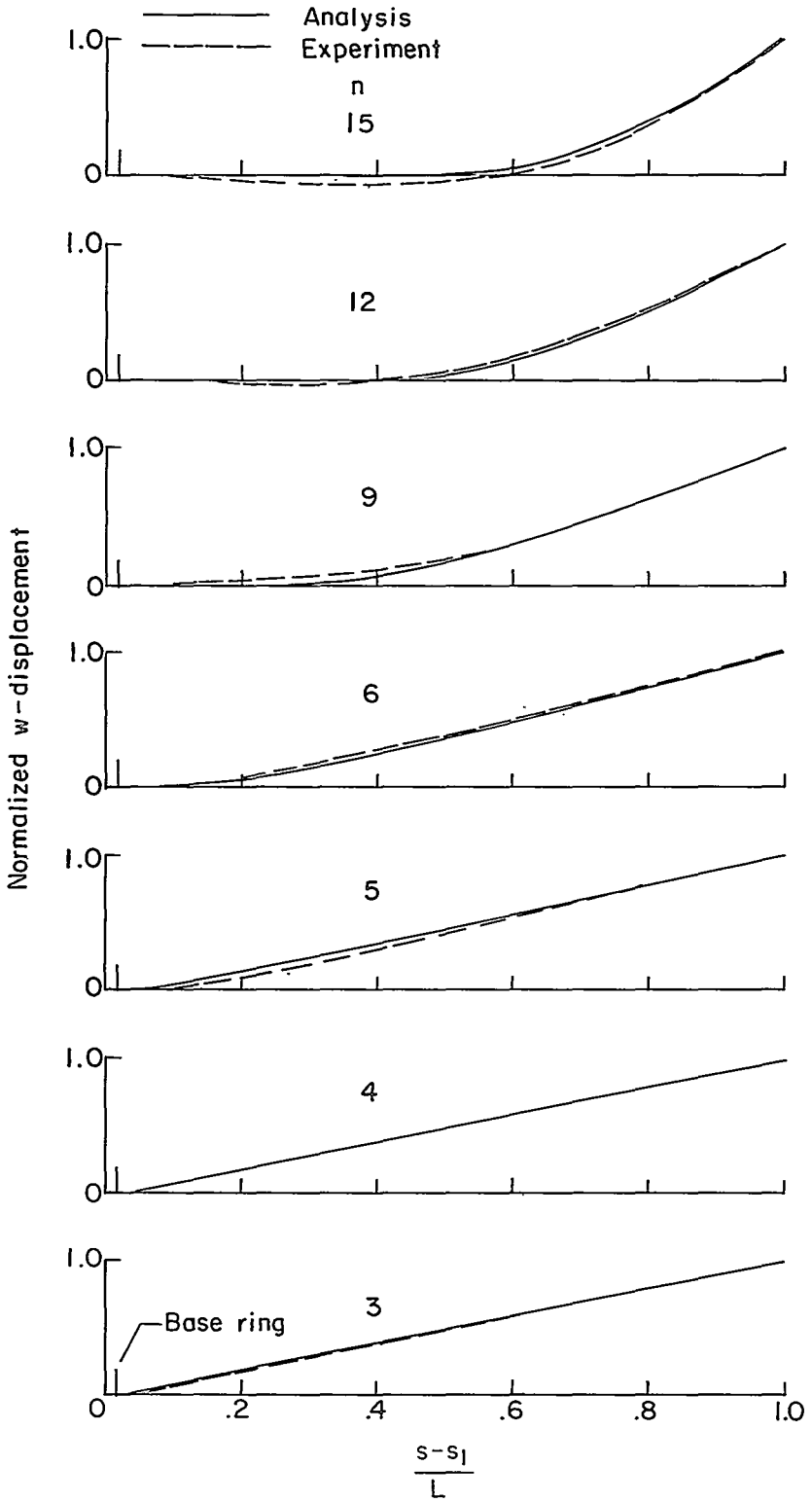

Figure 3.- Meridional mode shapes of 60° clamped-free conical shell with base ring.

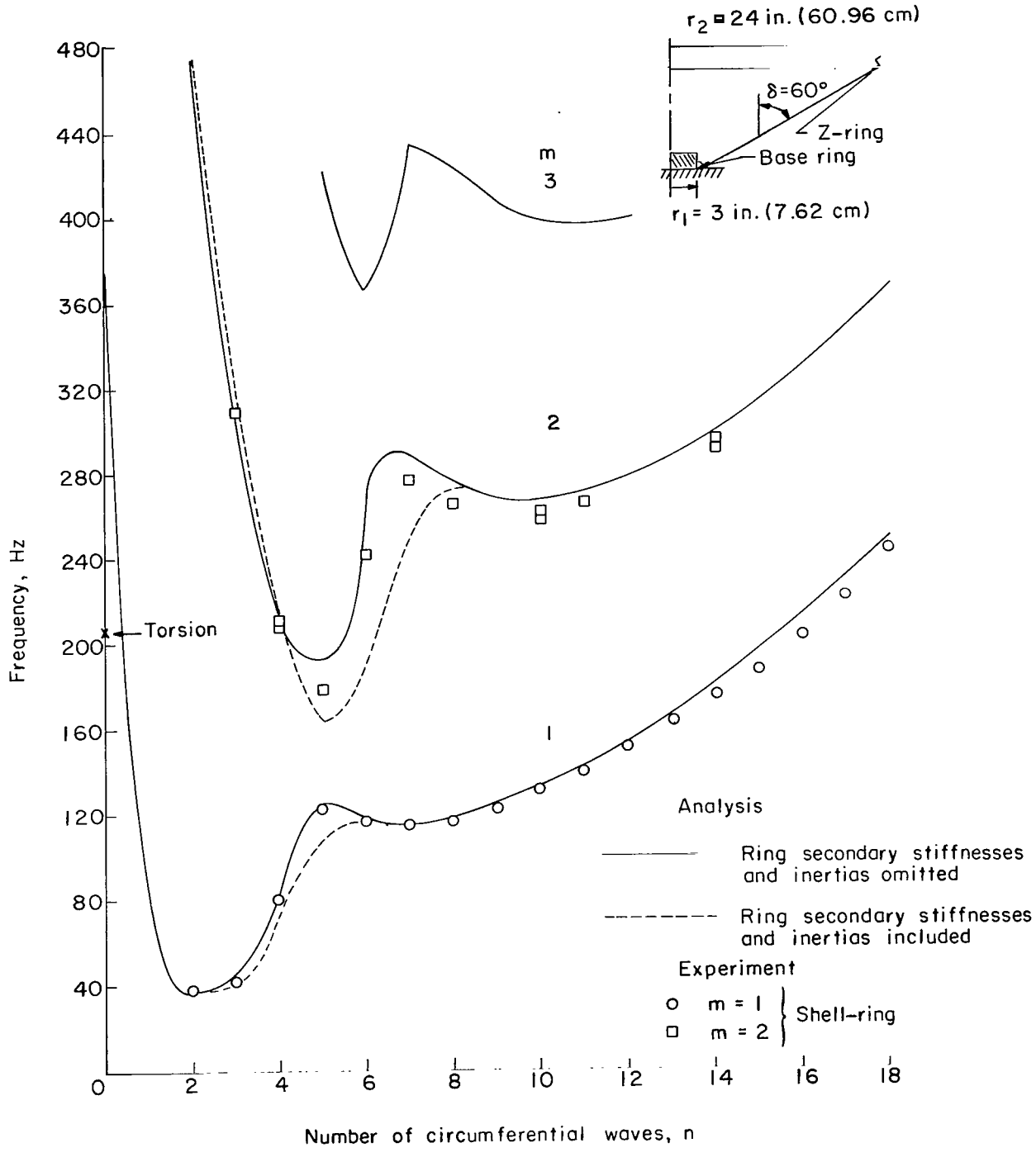

(a) Experimental frequencies and analytical frequencies based on primary ring stiffnesses.

Figure 4.- Frequencies of 60^0 clamped-free conical shell with base ring and Z-ring at free end.

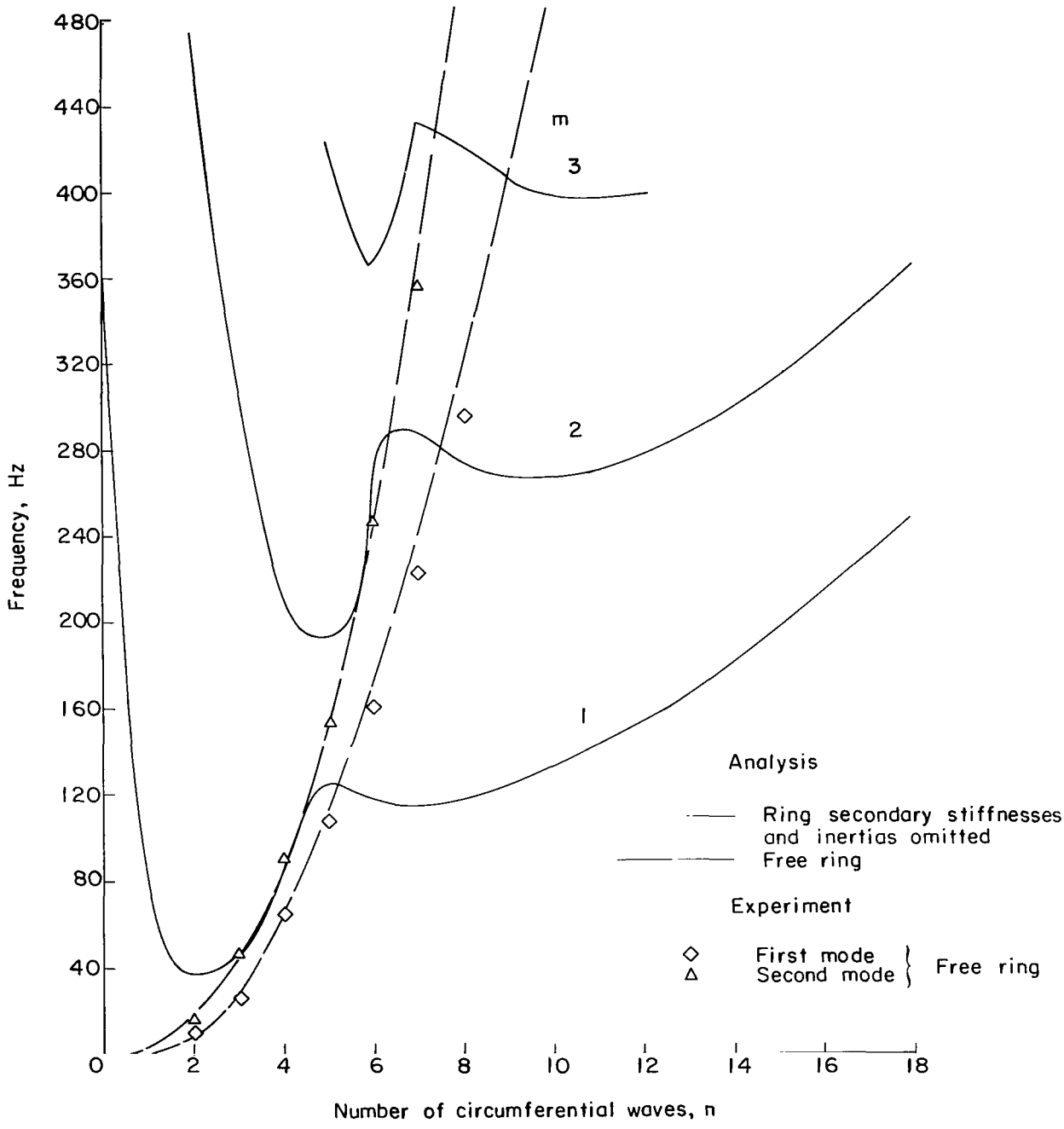

(b) Comparison of analytical shell-ring frequencies and free-ring frequencies.

Figure 4.- Continued.

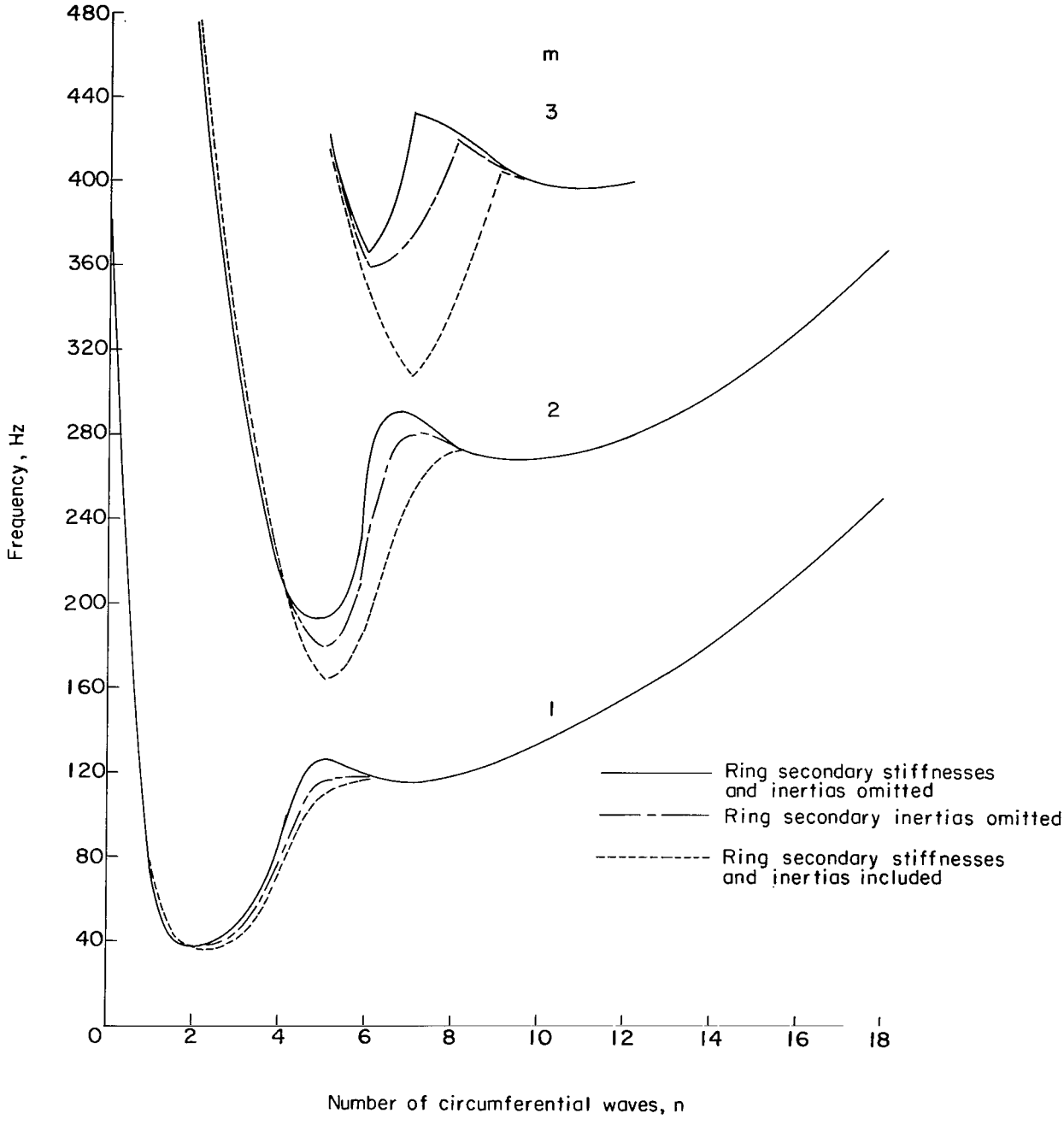

(c) Effects of ring secondary stiffnesses and inertias.

Figure 4.- Concluded.

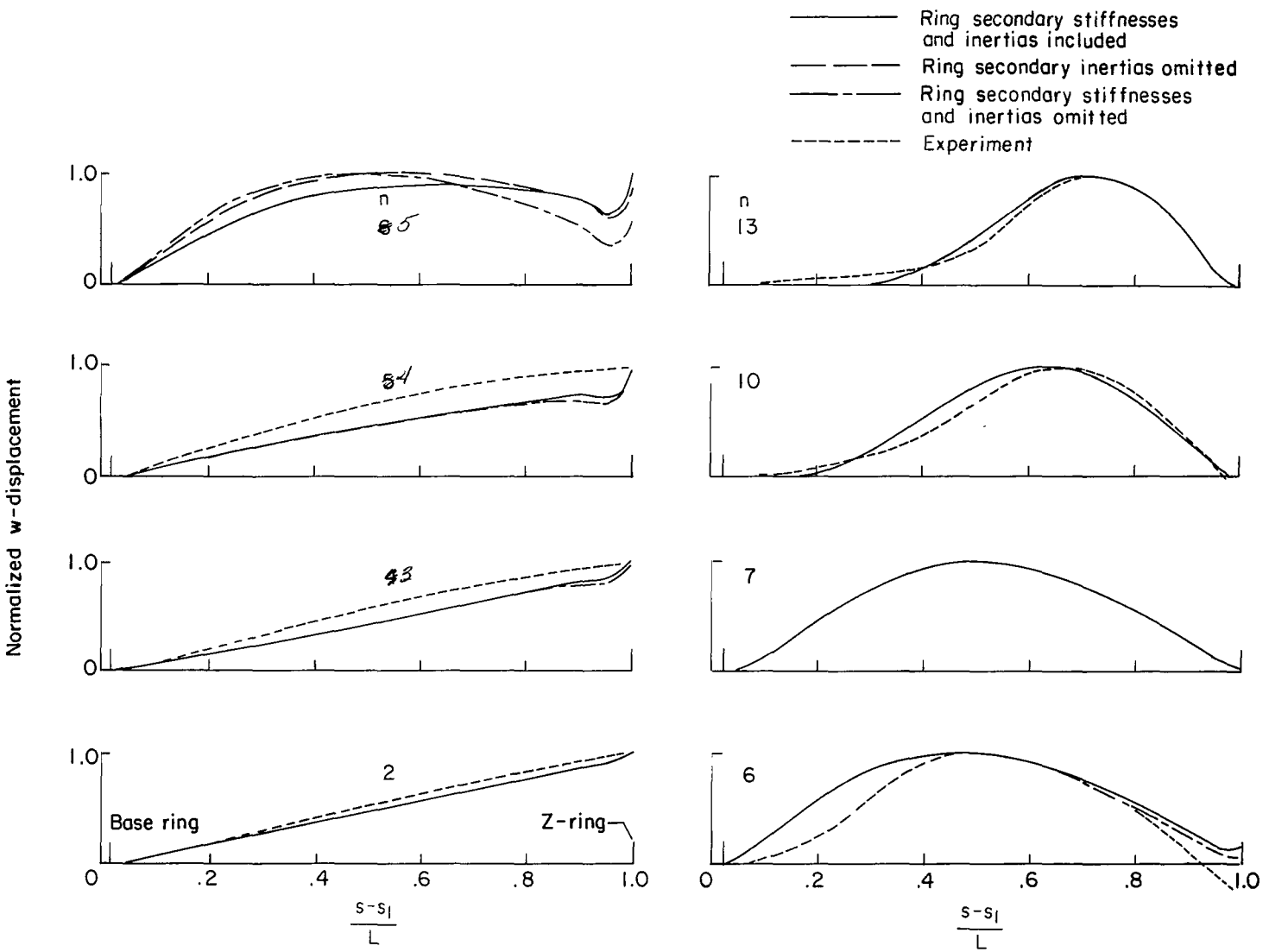

(a) m = 1.

Figure 5.- Meridional mode shapes of 60^0 clamped-free conical shell with base ring and Z-ring at free end.

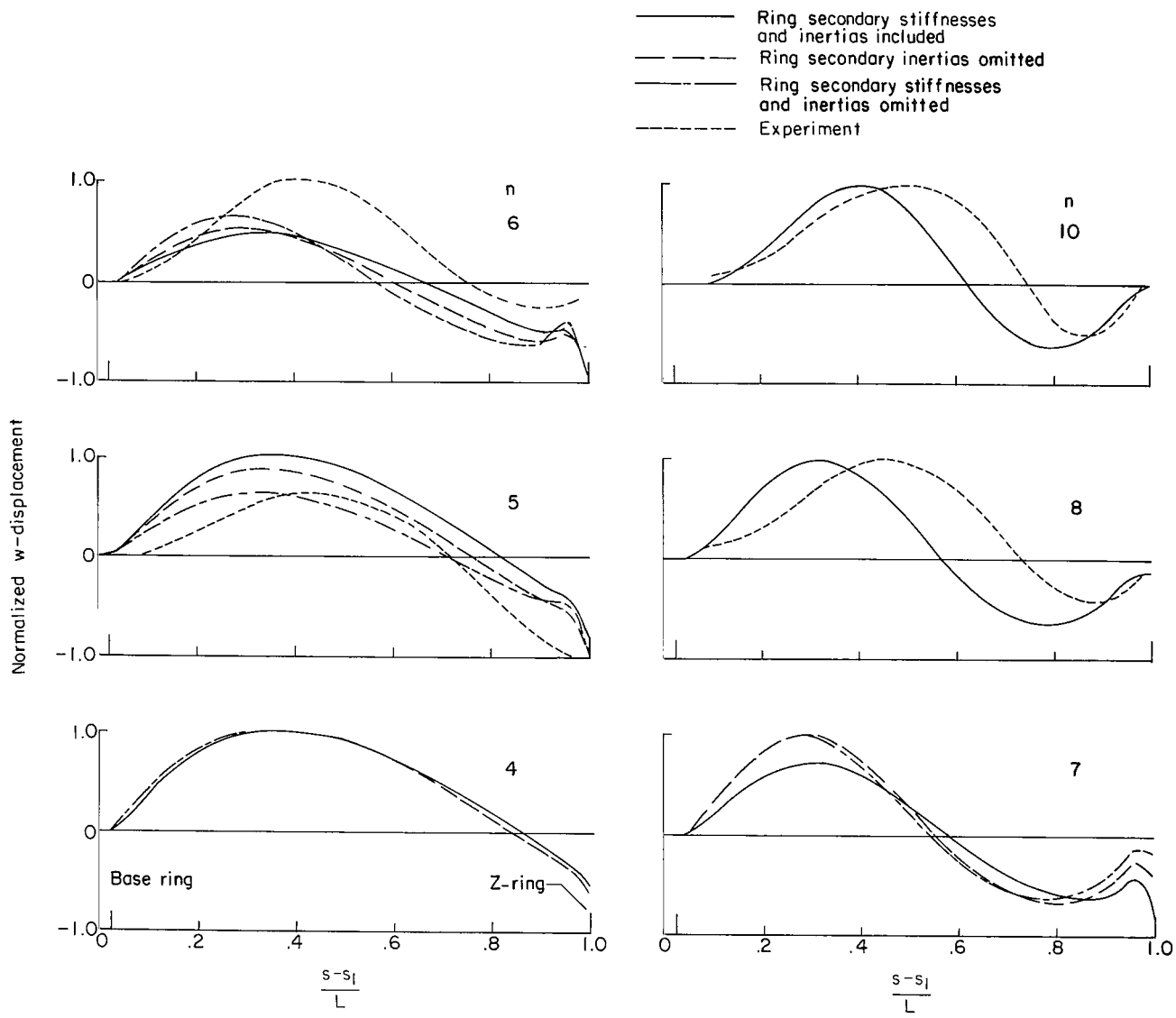

(b) m = 2.

Figure 5.- Continued.

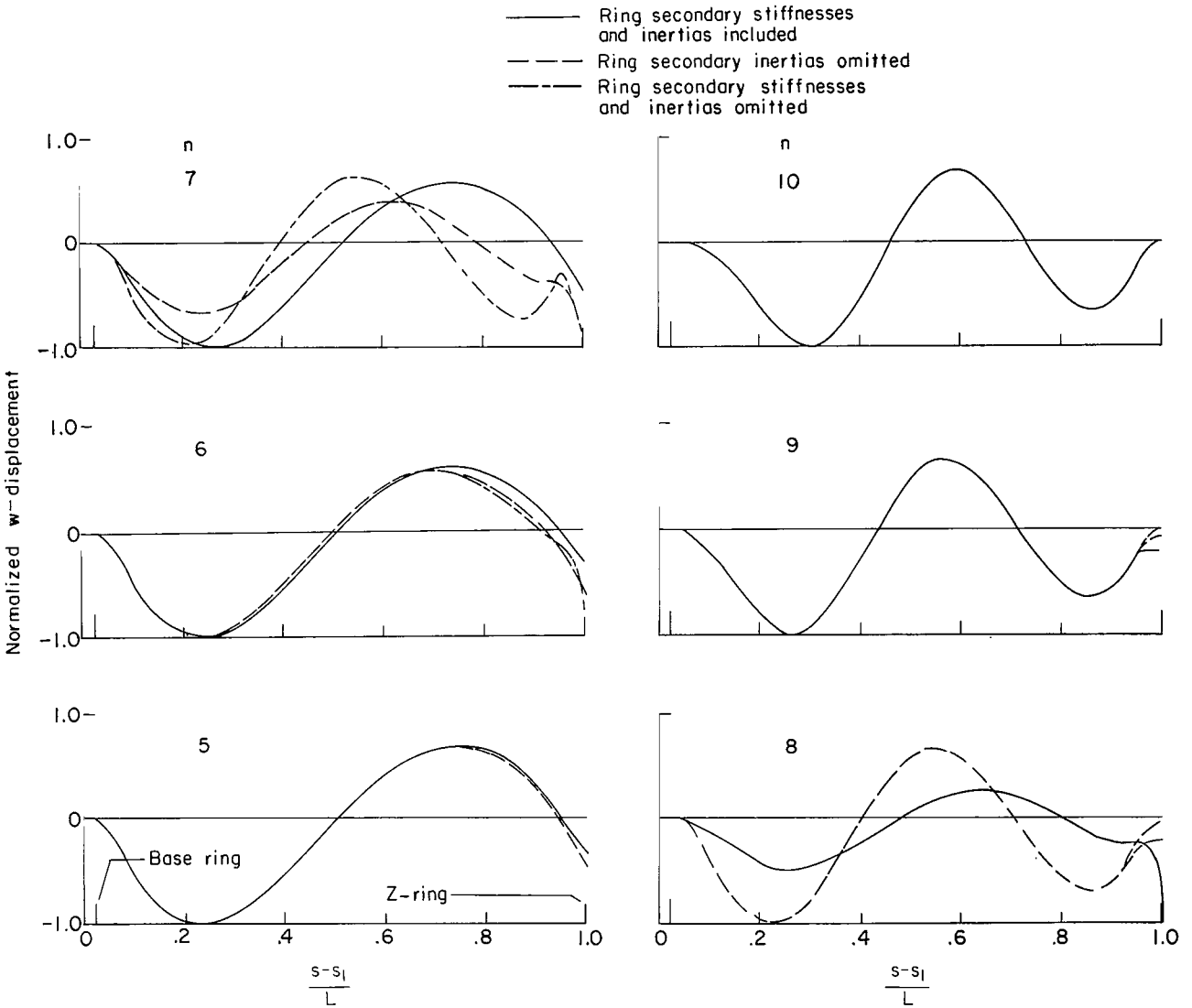

(c) m = 3.

Figure 5.- Concluded.

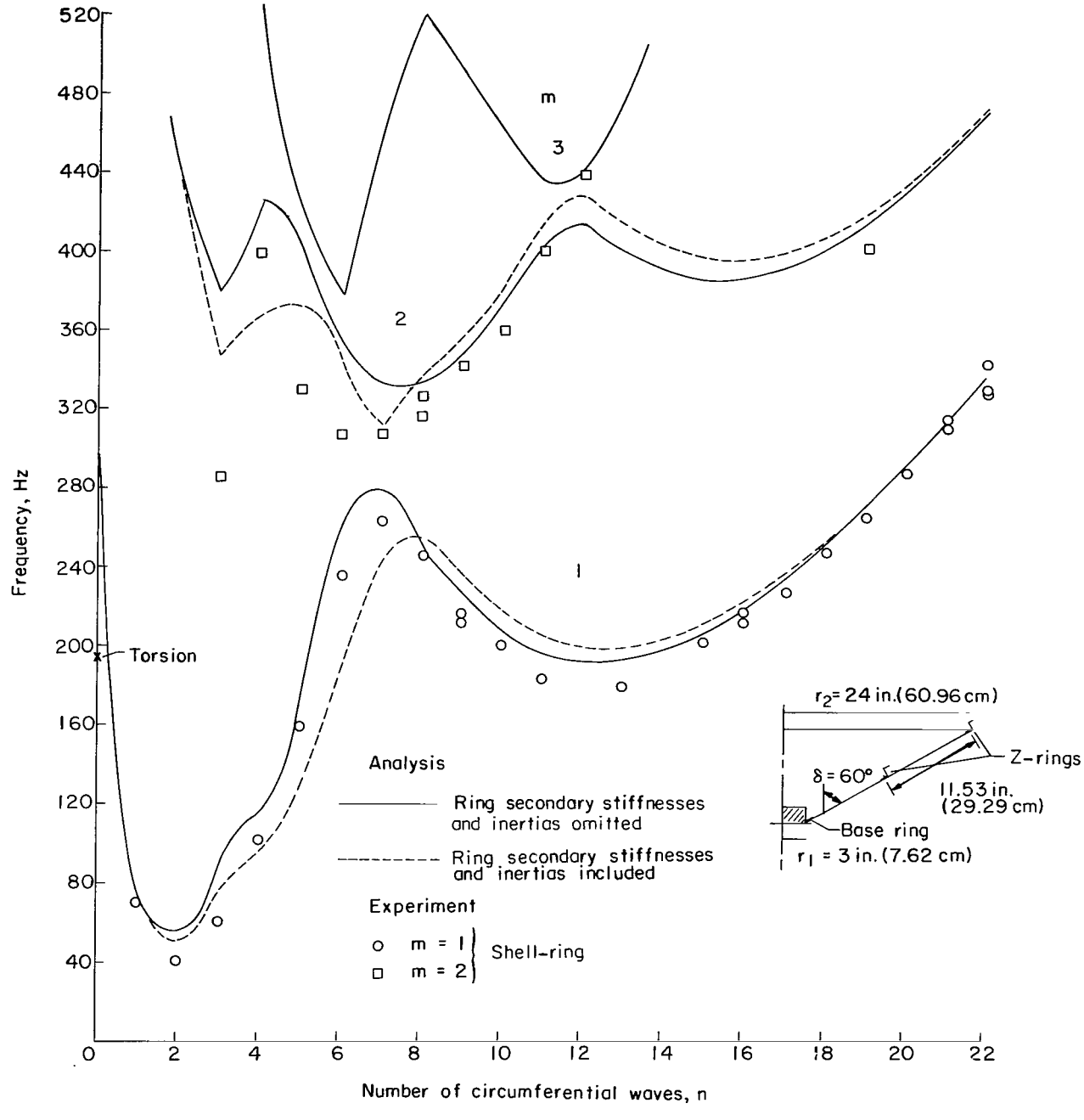

(a) Experimental frequencies and analytical frequencies based on primary ring stiffnesses.

Figure 6.- Frequencies of 60^0 clamped-free conical shell with base ring and two Z-rings.

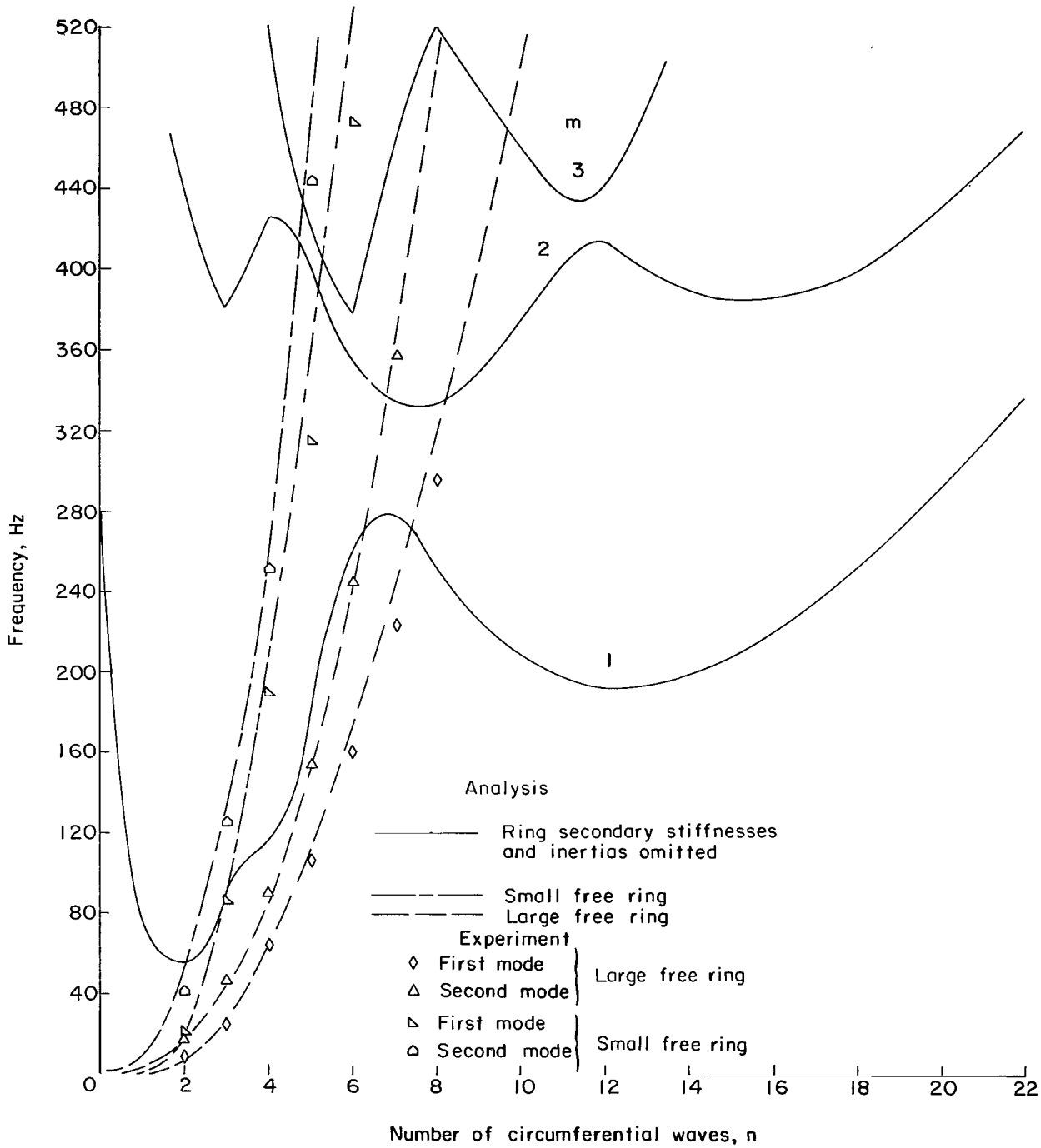

(b) Comparison of analytical shell-ring frequencies and free-ring frequencies.

Figure 6.- Continued.

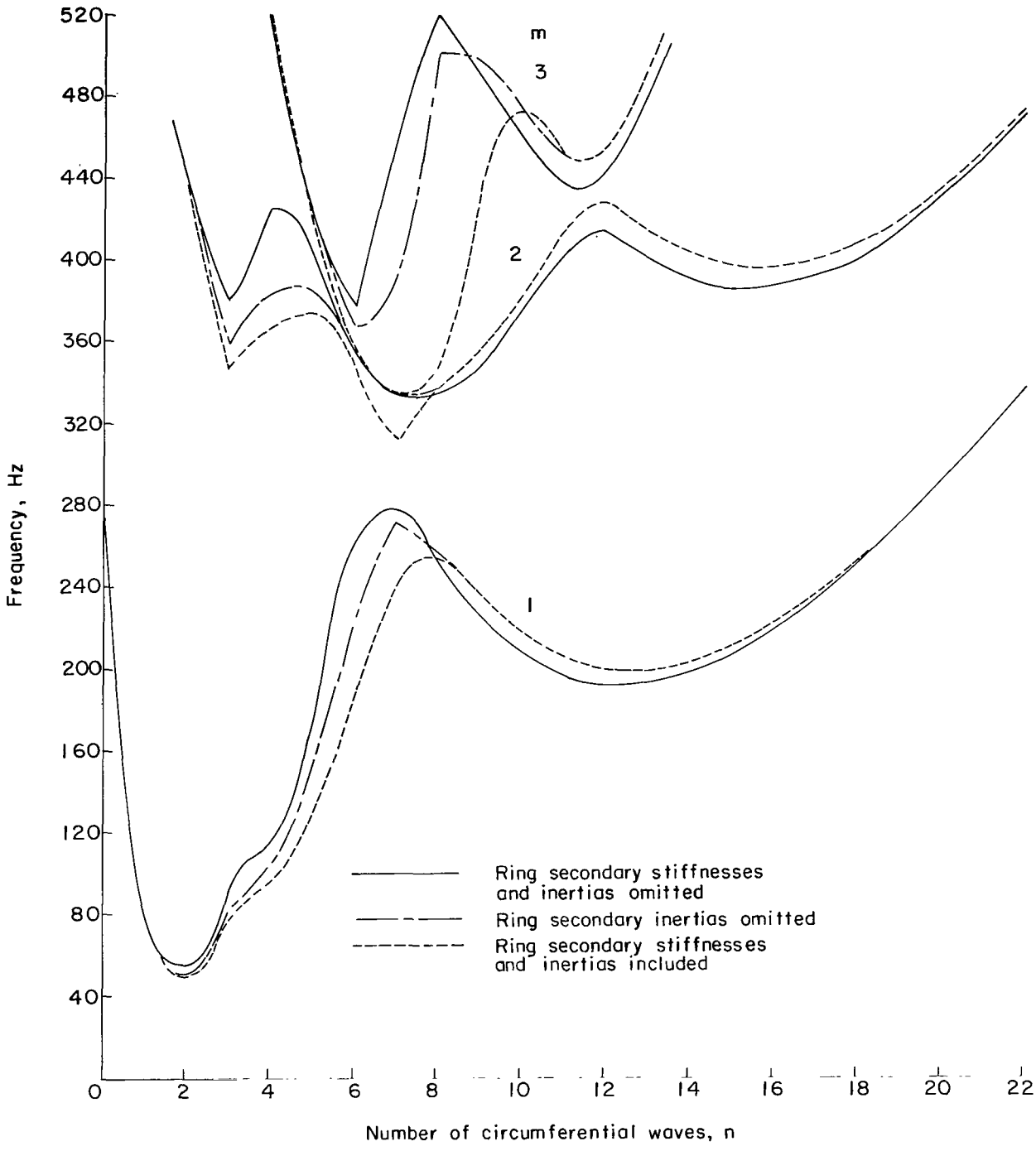

(c) Effects of ring secondary stiffnesses and inertias.

Figure 6.- Concluded.

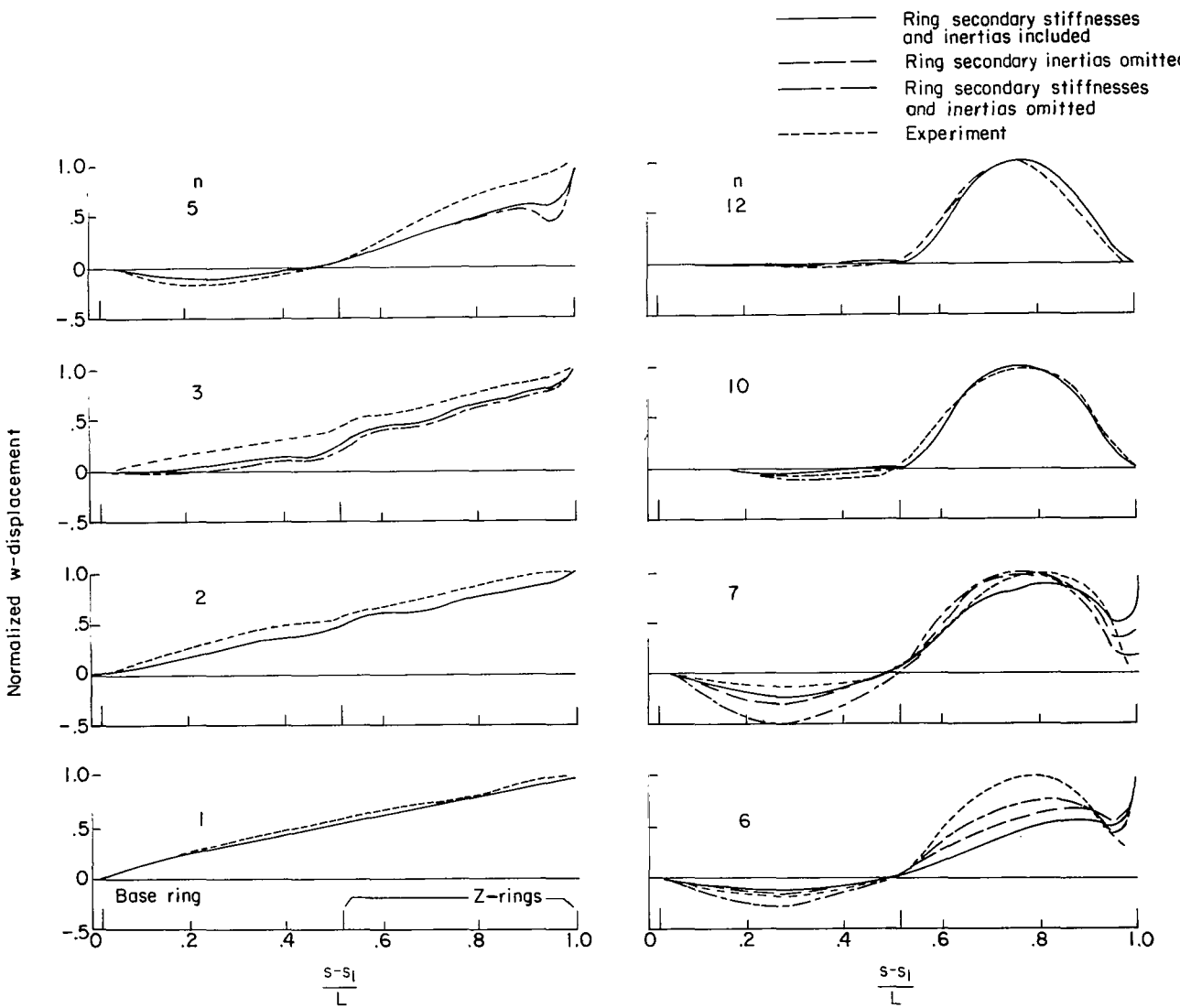

(a) m = 1.

Figure 7.- Meridional mode shapes of 60° clamped-free conical shell with base ring and two Z-rings.

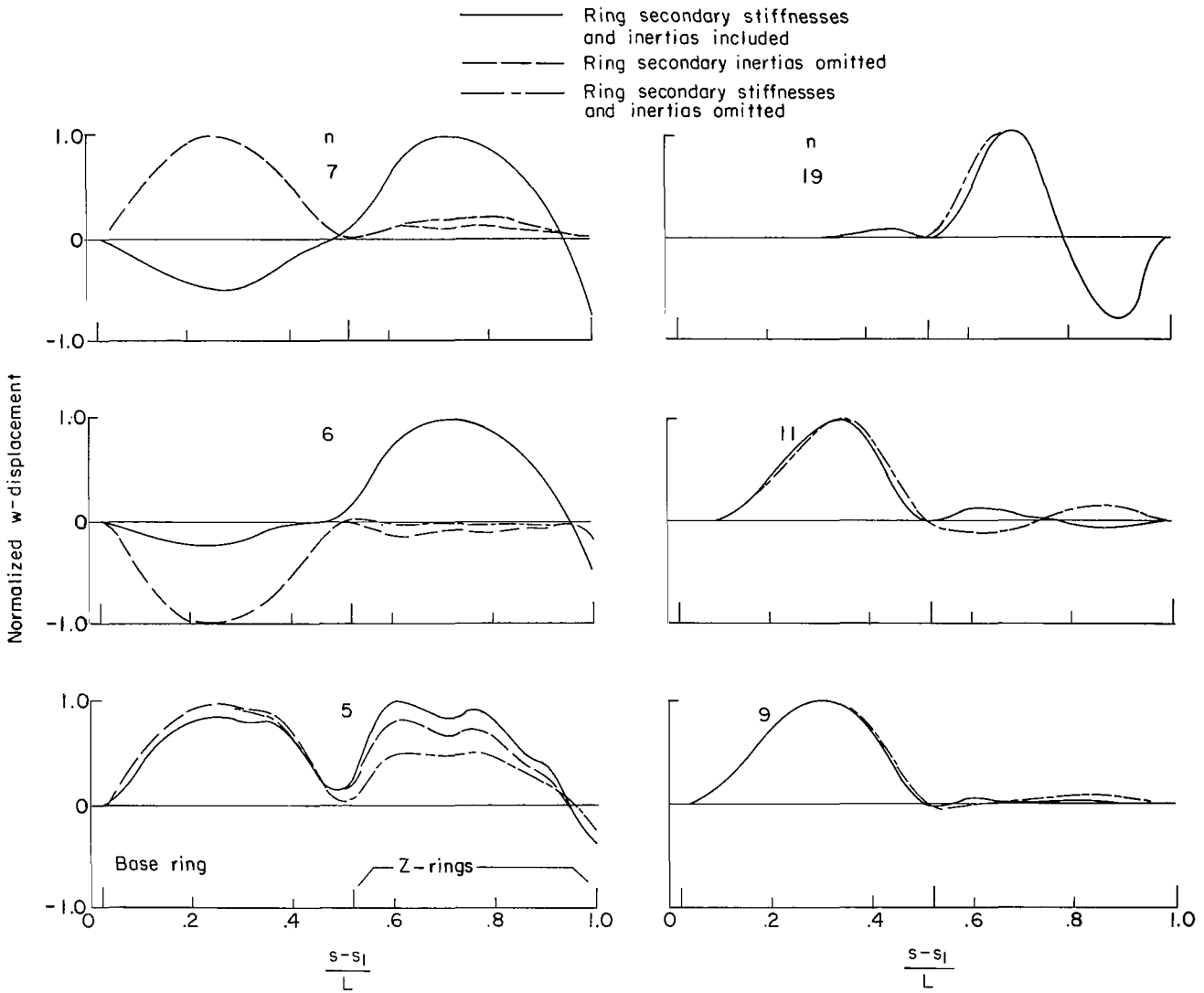

(b) m = 2.

Figure 7.- Continued.

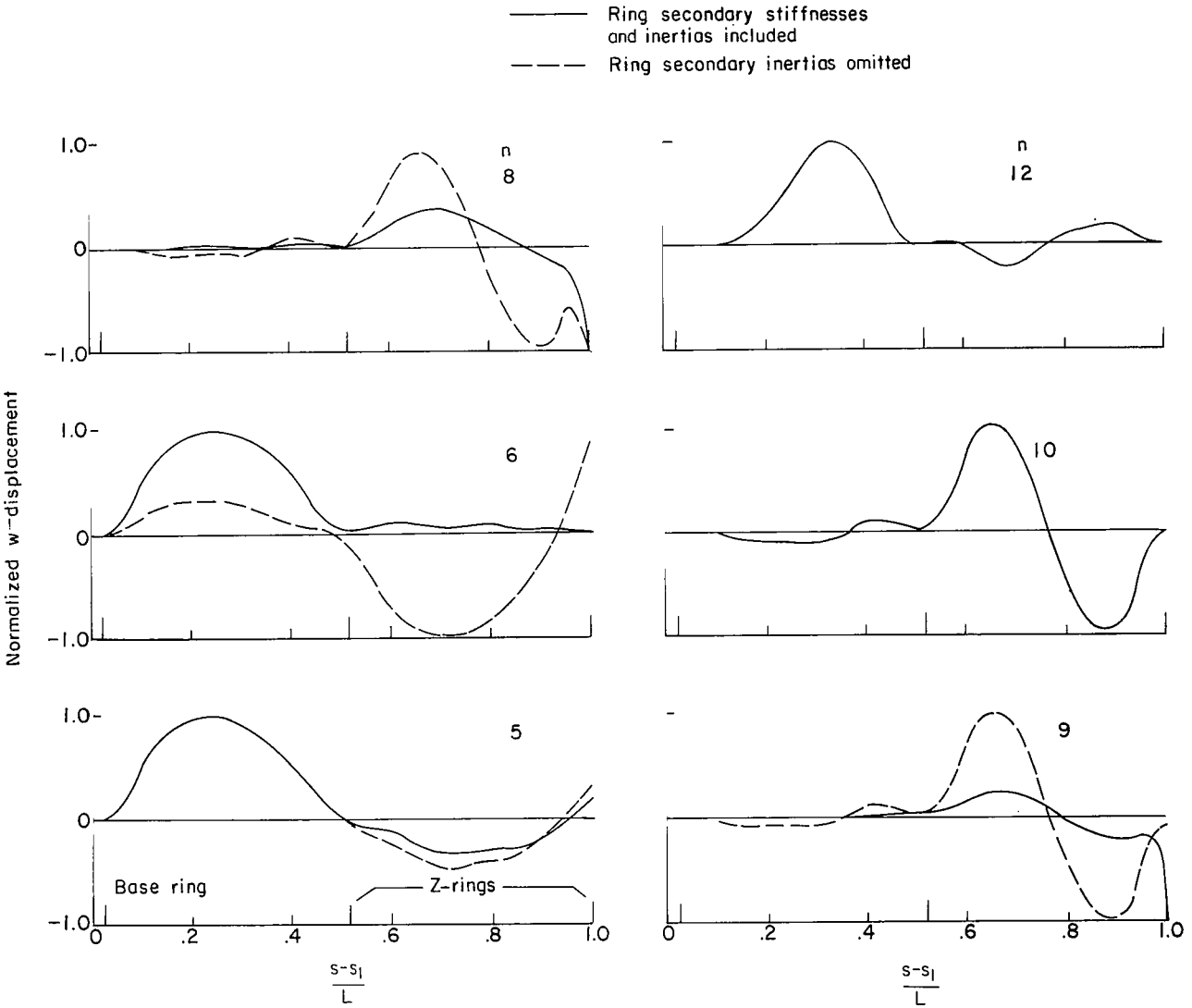

(c) m = 3.

Figure 7.- Concluded.

"The aeronautical and space activities of the United States shall be conducted so as to contribute . . . to the expansion of human knowledge of phenomena in the atmosphere and space. The Administration shall provide for the widest practicable and appropriate dissemination of information concerning its activities and the results thereof."

—NATIONAL AERONAUTICS AND SPACE ACT OF 1958

NASA SCIENTIFIC AND TECHNICAL PUBLICATIONS

TECHNICAL REPORTS: Scientific and technical information considered important, complete, and a lasting contribution to existing knowledge.

TECHNICAL NOTES: Information less broad in scope but nevertheless of importance as a contribution to existing knowledge.

TECHNICAL MEMORANDUMS: Information receiving limited distribution because of preliminary data, security classification, or other reasons.

CONTRACTOR REPORTS: Scientific and technical information generated under a NASA contract or grant and considered an important contribution to existing knowledge.

TECHNICAL TRANSLATIONS: Information published in a foreign language considered to merit NASA distribution in English.

SPECIAL PUBLICATIONS: Information derived from or of value to NASA activities. Publications include conference proceedings, monographs, data compilations, handbooks, sourcebooks, and special bibliographies.

TECHNOLOGY UTILIZATION PUBLICATIONS: Information on technology used by NASA that may be of particular interest in commercial and other non-aerospace applications. Publications include Tech Briefs, Technology Utilization Reports and Notes, and Technology Surveys.

Details on the availability of these publications may be obtained from:

SCIENTIFIC AND TECHNICAL INFORMATION DIVISION

NATIONAL AERONAUTICS AND SPACE ADMINISTRATION

Washington, D.C. 20546